Journal of Volcanology and Geothermal Research 265 (2013) 60–77

Contents lists available at ScienceDirect

Journal of Volcanology and Geothermal Research

journal homepage: www.elsevier.com/locate/jvolgeores

Volcanic evolution of the South Sandwich volcanic arc, South Atlantic, from multibeam bathymetry

Philip T. Leat [a,b,*], Simon J. Day [c], Alex J. Tate [a], Tara J. Martin [a,d], Matthew J. Owen [e], David R. Tappin [f]

[a] British Antarctic Survey, High Cross, Madingley Road, Cambridge CB3 0ET, UK
[b] Department of Geology, University of Leicester, University Road, Leicester LE1 7RH, UK
[c] Aon Benfield UCL Hazard Research Centre, Department of Earth Sciences, University College London, 136 Gower Street, London WC1E 6BT, UK
[d] CSIRO National Marine Facility, Castray Esplanade, Hobart, Tasmania, Australia
[e] Department of Geography, University College London, 136 Gower Street, London WC1E 6BT, UK
[f] British Geological Survey, Keyworth, Nottingham NG12 5GG, UK

ARTICLE INFO

Article history:
Received 1 May 2013
Accepted 24 August 2013
Available online 4 September 2013

Keywords:
Volcanic arc
Subduction zone
Caldera
Seamount
Submarine volcanism

ABSTRACT

New multibeam bathymetry data are presented for the South Sandwich intra-oceanic arc which occupies the small Sandwich plate in the South Atlantic, and is widely considered to be a simple end-member in the range of intra-oceanic arc types. The images show for the first time the distribution of submarine volcanic, tectonic and erosional–depositional features along the whole length of the 540 km long volcanic arc, allowing systematic investigation of along-arc variations. The data confirm that the volcanic arc has a simple structure composed of large volcanoes which form a well-defined volcanic front, but with three parallel cross-cutting seamount chains extending 38–60 km from near the volcanic front into the rear-arc. There is no evidence for intra-arc rifting or extinct volcanic lines. Topographic evidence for faulting is generally absent, except near the northern and southern plate boundaries. Most of the volcanic arc appears to be built on ocean crust formed at the associated back-arc spreading centre, as previously proposed from magnetic data, but the southern part of the arc appears to be underlain by older arc or continental crust whose west-facing rifted margin facing the back-arc basin is defined by the new bathymetry. The new survey shows nine main volcanic edifices along the volcanic front and ca. 20 main seamounts. The main volcanoes form largely glaciated islands with summits 3.0–3.5 km above base levels which are 2500–3000 m deep in the north and shallower at 2000–2500 m deep in the south. Some of the component seamounts are interpreted to have been active since the last glacial maximum, and so are approximately contemporaneous with the volcanic front volcanism. Seven calderas, all either submarine or ice-filled, have been identified: Adventure volcano, a newly discovered submarine volcanic front caldera volcano is described for the first time. All but one of the calderas are situated on summits of large volcanoes in the southern part of the arc, and most are associated with current or historic volcanic or hydrothermal activity. Shallow shelves around the islands are generally 1–10 km wide. Submerged banks up to 1100 m deep are interpreted as subsided erosional surfaces. Seamounts and emergent volcanoes experienced a range of mass wasting processes including by landsliding and smaller mass flows.

1. Introduction

The South Sandwich volcanic arc, situated in the South Atlantic (Fig. 1), is a tectonically simple, active, intra-oceanic arc, and is ideally suited to studies of volcanic arc crustal structure, geochemical investigation of mantle processes above a subduction zone, and sedimentation in an early stage of arc evolution. The active arc is built largely on oceanic crust of the small Sandwich plate which formed about 10 Ma at the back-arc East Scotia ridge spreading centre (Larter et al., 2003). The arc is forming in response to steeply inclined subduction of the South American plate beneath the Sandwich plate at the rate of 67–79 km/Ma (Thomas et al., 2003). It is relatively free of complicating factors such as intra-arc rifting, the presence of remnant arcs, or collision with seamount chains, oceanic plateaux or ridges. All the sediment arriving at the trench on the South American plate is subducted, and there is no accretionary prism (Vanneste and Larter, 2002).

For all these reasons, therefore, the South Sandwich volcanic arc is commonly viewed as representative of the "simple" or "primitive" end-member in the spectrum of intra-oceanic island arc systems (Baker, 1968; Wilson, 1989; Pearce et al., 1995). However, until the programme of seabed mapping and associated investigations discussed here was carried out, there had been no systematic study of the submarine morphology and structure of the arc. Therefore, it was not known if

* Corresponding author. Tel.: +44 1223 221432; fax: +44 1223 221646.
E-mail addresses: ptle@bas.ac.uk (P.T. Leat), simonday_ucl@yahoo.co.uk (S.J. Day), T.Martin@csiro.au (T.J. Martin), m.owen@ucl.ac.uk (M.J. Owen), drta@bgs.ac.uk (D.R. Tappin).

0377-0273/$ – see front matter © 2013 Elsevier B.V. All rights reserved.
http://dx.doi.org/10.1016/j.jvolgeores.2013.08.013

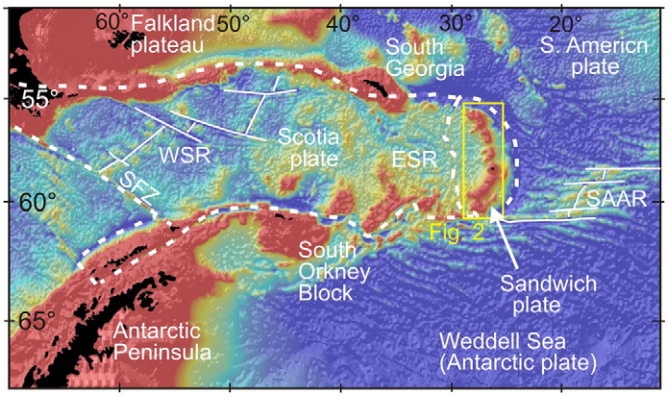

Fig. 1. Sketch map of the Scotia Sea showing the tectonic position of the Sandwich plate. Data are gravity-derived bathymetry. Tectonic boundaries of the Scotia and Sandwich plates are shown by white dashed lines. The extinct West Scotia Ridge (WSR) and active South America–Antarctica Ridge (SAAR) are shown by solid white lines. The Scotia and Sandwich plates are spreading apart at the East Scotia Ridge (ESR). SFZ, Shackleton Fracture Zone.

the subaerial volcanoes previously sampled and studied were representative of the whole of the arc or if the arc itself did not entirely conform to its own supposed "end-member" characteristics. It was not known if there were systematic along-arc variations in volcano morphology and structure, such as the development of submarine volcanic vents or submarine calderas, or submarine seamount volcanism in the fore- or rear-arc regions along cross-arc structures as seen in some other arcs. It was also not known whether submerged remnants of older arcs or displaced blocks of continental crust existed, especially along the northern and southern ends of the arc where it curves into transform fault zones known to contain such blocks. In this paper, we address these questions using the first comprehensive seabed mapping of the entire length of the South Sandwich arc. This paper presents hull-mounted multibeam echo sounder data which nearly completes bathymetric coverage of the volcanic arc.

The South Sandwich subduction zone may also be significant with respect to natural hazards and to the ecosystems of the Southern Ocean. The subduction zone is seismogenic but its potential for producing giant earthquakes is unknown. Should such earthquakes occur, the resulting tsunamis have the potential to be hazardous to South American and African coastlines (Dragani et al., 2009; Okal and Hartnady, 2009), especially in view of the present lack of tsunami sensors close to the arc. Tsunami risk from volcano slope failure in the island arc is present, but as yet unquantified. The volcanic arc is important biologically, as it hosts abundant marine life and sea bird colonies, and has a surprisingly rich benthic fauna (Kaiser et al., 2008). Distal ash falls, subglacial water discharges and sediment plumes, and sea level hydrothermal discharges from the South Sandwich arc are all potential sources of micronutrient element supplies to the surface layer of the Southern Ocean. Newly found seamounts are likely to be biodiversity hotspots, especially where hydrothermally active. New discoveries of submarine hydrothermal vents with associated communities in the back-arc and arc are among the most remote in the World's oceans (Rogers et al., 2012).

All the volcanoes forming the curved volcanic front are recently volcanically active or currently hydrothermally active, or both (Gass et al., 1963; Holdgate, 1963; Baker, 1990; Lachlan-Cope et al., 2001; Leat et al., 2003; Patrick et al., 2005; Patrick and Smellie, 2013). Even within the short period (less than 100 years) of historical records, eruptions from the South Sandwich arc have been varied, ranging from submarine explosive eruptions (Protector Shoal, 1962) through strombolian eruptions with associated lava flows (Montagu Island, 2001–2007 and Bristol Island, 1956), to possible lava lake activity (Saunders Island, 1995–1998).

The sub-Antarctic islands of the South Sandwich arc are small, the largest being Montagu which is 12 km across (Fig. 2). They are mainly ice-covered, and almost entirely devoid of vegetation. The extent of ice cover on the islands increases with latitude and height, and the large southern Islands, Montagu, Bristol, and Cook and Thule islands of the Southern Thule group, are heavily glaciated. Rates of erosion of the islands by a combination of glacial and coastal processes are probably high compared to other intra-oceanic arcs, and the resultant high sediment supply is thought to have led to the development of relatively prominent and large sediment wave fields on the submarine flanks of the islands (Leat et al., 2010a). We briefly comment upon further occurrences of sediment waves in newly-surveyed areas described in this paper, but their development and mechanisms of formation will be discussed in detail elsewhere.

There are seven large volcanoes along the curved volcanic front that emerge above sea level to form islands. These islands represent a small fraction of the volume of their respective volcanoes, which are very largely submarine. In a previous paper, Leat et al. (2010a) used multibeam data to document the submarine volcanic and sedimentological features of most of the northern part of the volcanic arc. Multibeam data have also been obtained for the submerged Douglas Strait Caldera on Southern Thule (Allen and Smellie, 2008), and Kemp seamount and the adjacent Kemp caldera (Supplementary Material S1). The East Scotia Ridge back-arc spreading centre and a section of the fore-arc have been mapped using the lower resolution towed Hawaii MR1 sonar (Livermore et al., 1997; Vanneste and Larter, 2002; Livermore, 2003). Previous sounding data are shown on the UK Admiralty Chart (Hydrographic Office, 2003), which was an invaluable route-finder during the survey work.

In this paper, we present multibeam data for the previously unsurveyed remainder of the volcanic arc, including the submarine parts of volcanoes that emerge as Saunders, Montagu and Bristol islands and the Southern Thule island group, a newly discovered volcanic front volcano named Adventure in the southern part of the arc, and the seamount cluster around Nelson Seamount. In addition we present data for parts of the area around Protector Shoal not previously surveyed. We compare these data with those from the northern part of the arc (Leat et al., 2010a), to allow us to examine trends along the length of the arc.

2. Methodology

The bathymetric data were acquired during two cruises (Supplementary Material S1). The northern part of the arc was investigated during 7-day cruise JR168 (NERC Cruise leg JR20070418) on British research ship RRS *James Clark Ross* in April–May 2007. These data were reported in Leat et al. (2010a). The new data that form the main basis for this paper were acquired from the same ship during 21 days in January–February 2010 on cruise JR206 (NERC Cruise leg JR20100118). The 2010 survey extended the area covered in 2007 in the northern part of Protector Seamounts, around Leskov Island, and the area from Saunders Island to the south of the arc (Fig. 2). Both cruises employed the same equipment and data acquisition methods. Bathymetric data were acquired using a hull-mounted Simrad EM 120 multibeam echo sounder. The system had a 12 kHz operating frequency and a 191 beam array with real-time beam steering and active pitch and roll compensation (Tate and Leat, 2007; Leat et al., 2010b). Data were acquired using Simrad's Merlin software and were cleaned manually using MB System v5.0.9 software. Cleaned data were gridded at 100 m horizontal resolution. Vertical measurement accuracy is in the order of 50 cm or 0.2% of depth RMS (whichever is greater). A number of new submarine volcanoes and other bathymetric features have been identified and informally named: the reasons for the choice of these names are discussed in Supplementary Material S2. Slope analysis used the 100 m resolution gridded data (Supplementary Material S3).

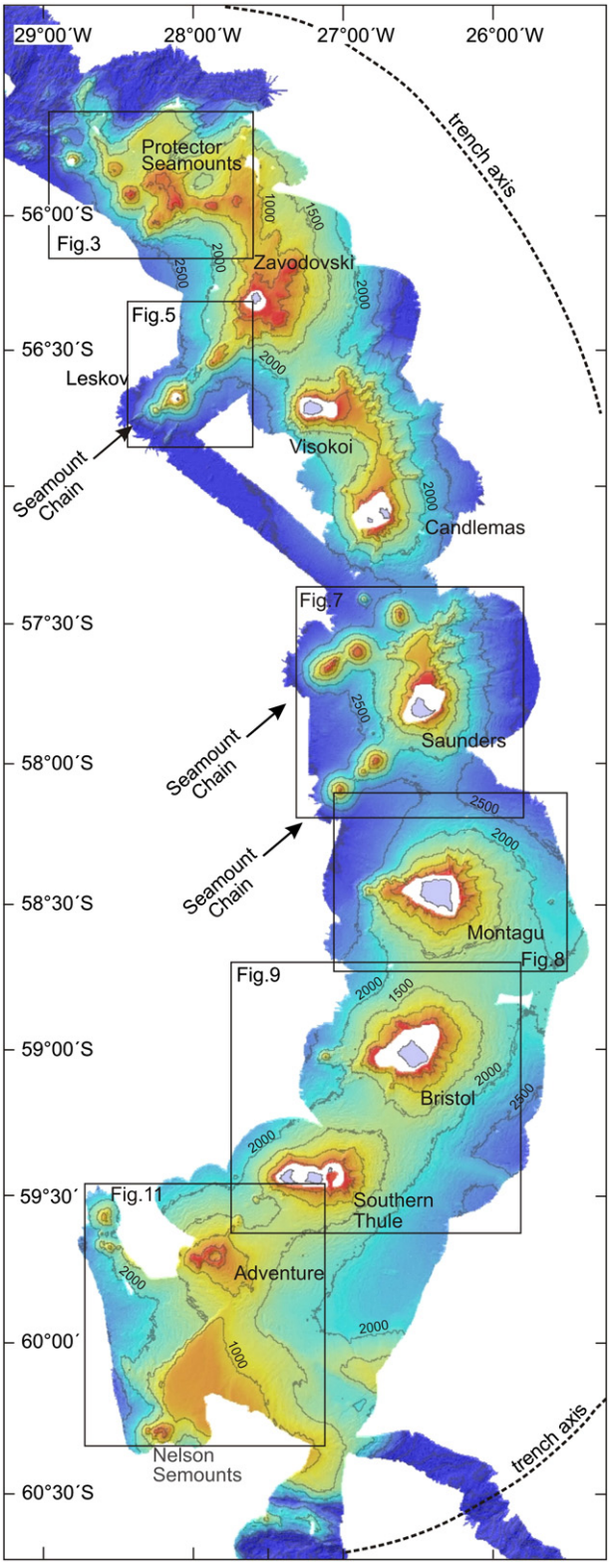

Fig. 2. Multibeam bathymetric map of the South Sandwich arc, showing data from cruises JR168 and JR206. Isobath interval 500 m.

3. Bathymetry of the South Sandwich arc

A compilation of multibeam bathymetric data from the 2007 and 2010 cruises is shown in Fig. 2. The combined survey extends over a north–south distance of 550 km, and is ca. 80–90 km wide. The map reveals much of the overall structure of the volcanic arc. The data coverage extends from above, or close to, shallow shelves around the islands to depths of some 2250–3000 m both east and west of the arc. The new coverage confirms that the volcanic arc has a relatively simple structure. There is a single main line of volcanoes, which form the currently active volcanic front. Evidence for extinct volcanic lines is absent. The simple structure is consistent with the relatively young age of the arc. Surface evidence for faulting is almost entirely absent, except in the proximity of the trench at both the north and south terminations of the arc, where it curves into the strike-slip plate boundaries and the back-arc spreading centre. There is no evidence for intra-arc rifting. Volcanoes in the southern part of the arc (Montagu, Bristol, Southern Thule) are larger and simpler, more conical structures than those in the northern part of the arc (Zavodovski, Visokoi, Candlemas and Saunders). Three cross-cutting seamount chains extend from NE to SW from the volcanic front for 50–70 km toward the rear-arc. We describe volcanism, structure and sedimentation in the arc from north to south.

3.1. Protector Seamounts

Protector Seamounts represent the northernmost volcanism in the volcanic arc. They form a generally east–west trend, although there are significant departures from a simple chain (Fig. 3). Most of the seamounts were described by Leat et al. (2010a), but bathymetric data collected in 2010 extends the coverage to the north. Samples obtained from the seamounts are dominantly silicic (Leat et al., 2007; authors' unpub. data, 2011). The new data show that Protector Seamounts coalesce to the north with a plateau, Nimrod Bank, which forms a central point within the seamount chain. The bank is 11.4 km across at the 750 m isobath with some ridges projecting further, and some 850 m high. Most of the Bank is 400–600 m deep and its surface is irregular, underlain by several domes 0.8–1.2 km across, one of which, 130 m high, forms its shallowest point at 365 m depth (summit dome in Fig. 3). Similar domes occur at 1100–1400 m depth between Nimrod Bank and Quest. Central parts of the Bank above 430 m are almost flat. Several depressions up to 60 m deep occur on the SW part of the Bank. The outer slopes of the Bank are smooth, generally slope at 13–20° and are nowhere incised. The Bank is interpreted as a volcanic plateau surmounted and flanked by volcanic domes. The lack of incision of the flanks and abundance of domes suggests that it is a relatively recent construct.

Several faults in the NE–SW trending cluster to the NE cut into the Bank and control Nimrod and Bisco basins, both some 10 km across. The NW slope of Nimrod Bank faces Nimrod Basin which extends NW toward the trench. Nimrod Basin is tectonically defined, like the enclosed Bisco Basin to the south. Faults along the margin extend on to Nimrod Bank, where the extensions of the faults form a NW-facing embayment on the summit of the bank (Fig. 4). The curved SE-facing side wall of this embayment is some 50 m high. The embayment may represent a landslide scar 2.8 km across formed during a collapse toward Nimrod Basin of a sector of the volcano summit. The prominent slump on the south flank of Protector Shoal extends 19 km from a 2.5 km wide bowl-like scar near the seamount summit to beyond the base of the seamount. The upper part of the slump is characterised by 100–340 m high back-rotated steps (Leat et al., 2010a).

3.2. Leskov Seamounts

This seamount chain forms a ridge that extends 60 km to the SW of Zavodovski (Fig. 2). Leskov Island is the highest point along the ridge, forming the only emergent part and the summit of the largest volcanic construct; Vostok and Mirnyi are the other main seamounts (Fig. 5). Leskov Island is ca. 900 m across and rises to 190 m above sea level. Its coastline consists entirely of cliffs (Holdgate and Baker, 1979) and the island dominantly comprises eroded andesite lava flows. There is no historic record of volcanic eruptions. Compositionally, the andesites

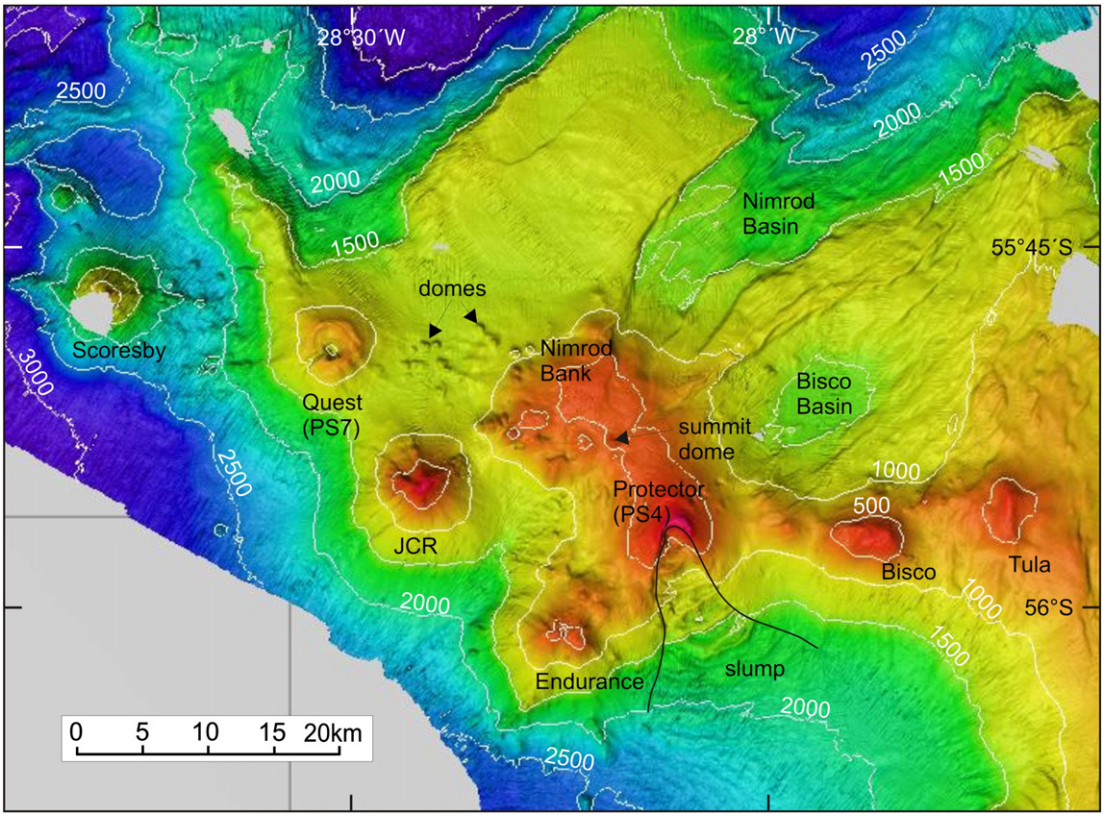

Fig. 3. Multibeam bathymetric map of Protector Seamounts. Isobath interval 500 m. The margins of the slump on the southeast face of Protector Shoal are indicated by the solid line. Names are unofficial and have been renamed from the PS1–PS7 usage of Leat et al. (2010a).

belong to the local 'calc-alkaline' series and have distinct rear-arc characteristics (Pearce et al., 1995; Tonarini et al., 2011).

Mirnyi Seamount is elongate along the SW-trending ridge rising to a plateau that is 10 km across. On the SE part of the plateau several minor ridges trend parallel to main ridge, and may be faults or eruption fissures (Fig. 6). The plateau is surmounted by several rounded mounds some 100–150 m high, including the 445 m deep summit (Figs. 5A, 6). All the mounds have lobate slopes of about 19–27° which coalesce to form much of the flanking slopes of the Mirnyi ridge and are interpreted as volcanic cones or domes. More lobate structures with steep downward facing slopes that occur at 2000–2500 m depth south of Mirnyi summit are interpreted as lava flows (Fig. 6). The cones, domes and lavas are interpreted to have been fed by a fissure system trending from ZW5 on the SW slopes of the Zavodovski edifice in a SW direction along the length of the ridge.

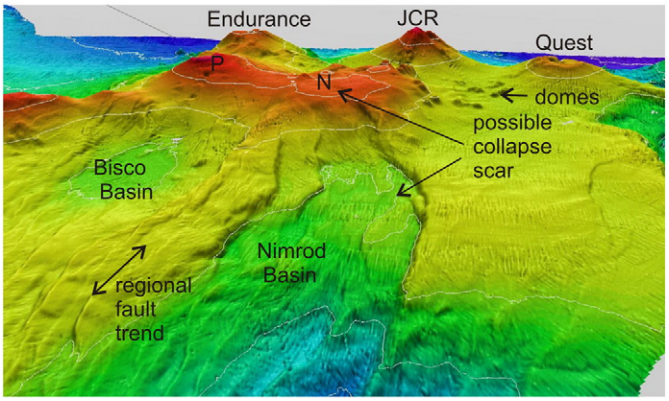

Fig. 4. Oblique image of Protector Seamounts viewed from the northeast. A possible collapse scar extends from the summit of Nimrod Bank toward the viewer into Nimrod Basin. P, Protector Shoal; N, Nimrod Bank.

The submarine part of the Leskov edifice forms an almost conical structure, rising from a base of around 2500 m below sea level. Its slopes are generally smooth and 17–23° above the 1000 m isobath. Its east-facing slope is cut by two embayments some 3 km long and 0.8 km wide (Fig. 6) which are interpreted as relatively small landslide scars.

Vostok Seamount is surmounted by a conical summit which rises to 1139 m below sea level from a base at about 2000 m depth. This conical summit is superimposed on a larger truncated cone that appears to have been modified by collapse. A large, prominent scar forms a 8 km diameter horseshoe that opens toward the SW, with inward-facing scarps that are highest directly south of the seamount, where they are up to 143 m high, reducing to ~76–100 m further from the summit. A 5 × 3 km area on the floor of this scar is occupied by a hummocky terrain containing irregular, unevenly distributed hillocks up to 75 m high and 300 m long (Fig. 5B). This terrain is interpreted as a proximal debris avalanche deposit (Siebert, 1984). The summit cone fills most of source horseshoe area of the collapse. Its SW-facing slope is cut by a second scar 2 km across interpreted as a later collapse.

3.3. Saunders

The bathymetric data show that Saunders is a large central edifice, and intersected by two seamount chains (Fig. 7A). The volcano is 55 km across at the 2500 m isobath, and generally conical, with Saunders Bank forming a large, dissected plateau extending to the north. Saunders Island (9.2 × 6.3 km) is dominated by its central ice-covered cone of Mount Michael (Fig. 7B) which has a ca. 500 m diameter summit crater (Patrick and Smellie, 2013). Satellite data suggest intermittent lava lake and tephra eruptions in this crater (Lachlan-Cope et al., 2001; Patrick and Smellie, 2013). The north part

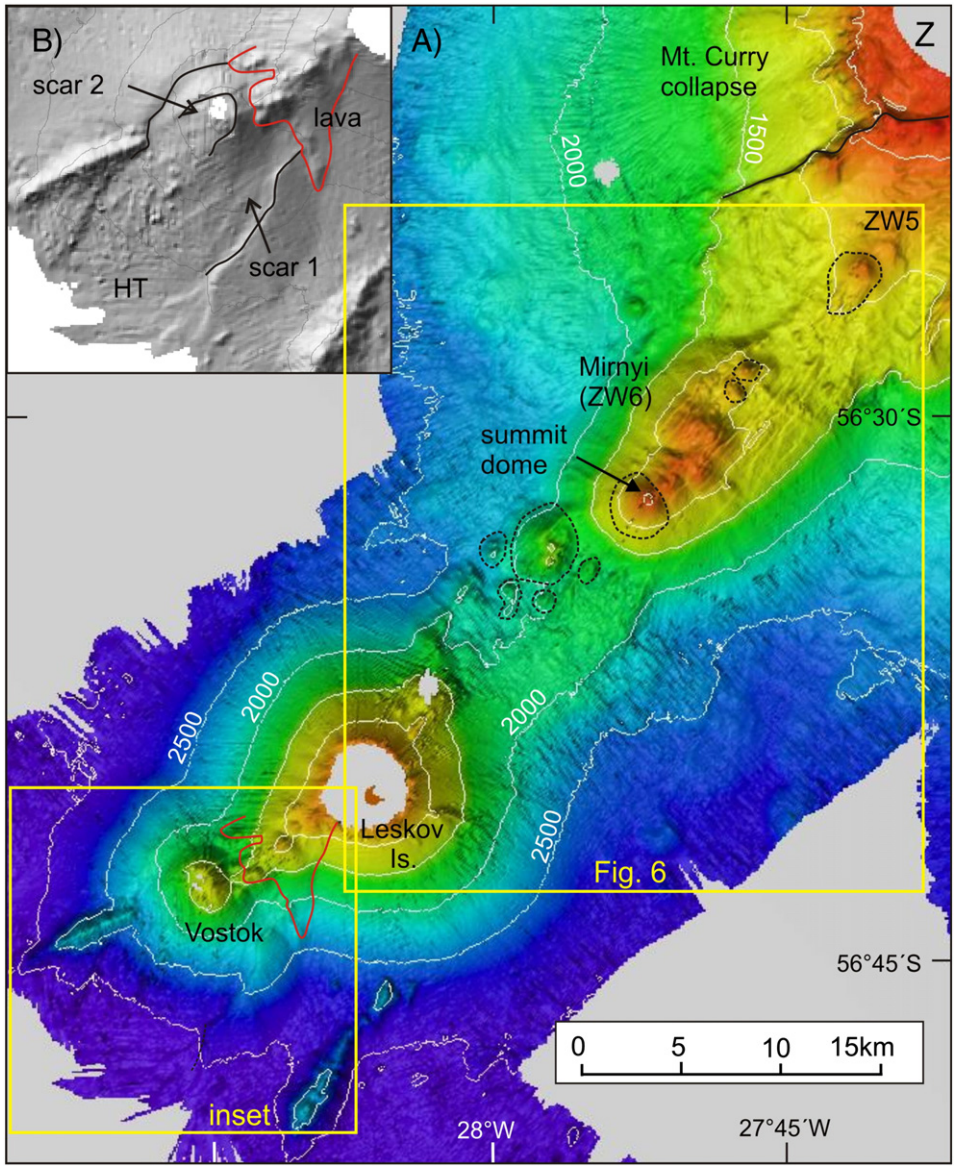

Fig. 5. Images of Leskov seamount chain. A. Multibeam bathymetry map. Isobath interval 500 m. Black solid lines indicate interpreted margins of collapse scars. The Mt. Curry collapse was derived from Zavodovski volcano (Z) to the top right of the image. Features ZW5 and ZW6 are described in the text. Dashed lines are outlines of volcanic cones/domes along the axis of the seamount chain. B. Hillshade image of Vostok Seamount. Black solid lines indicate interpreted margins of collapse scars. Two phases of collapse scars are imaged. Red line is interpreted lava flow front. HT, hummocky terrain.

of the island consists of young basaltic lavas that have surrounded former sea stacks at Yellowstone Crags (Holdgate and Baker, 1979, Fig. 7C). The NE coast of the island is occupied by the ca. 6 km wide Cordelia Bay which is shallow and has numerous reefs and sea stacks forming Brothers Rocks some 2 km offshore. Despite its semi-circular form, there is no evidence that it is a collapse scar or caldera.

The only part of the shallow shelf to be surveyed was to the north of the island where a shelf at least 4 km wide forms Harper Bank. The shelf is typically 150–200 m below sea level, containing indistinct east–west trending ridges visible on the slope analysis image (Supplementary Data Fig. S3.4). The depth of the shallow shelf close to the island is poorly known, but soundings suggest a depth of 30–50 m in Cordelia Bay (Hydrographic Office, 2003). To the north, Harper Bank slopes abruptly down to the flat 12 × 15 km Saunders Bank. This extensive bank slopes gently to the north from around 750 m near Harper Bank to about 1100 m at its northern edge. Both Harper and Saunders banks are strongly incised on their eastern margins. Ridges S1 to S3 (Fig. 7A) are interpreted as erosional remnants, suggesting that a pre-erosion Saunders Bank extended significantly farther east.

Ridge S4 extends some 19 km SE from Saunders (Fig. 7A). It is up to 300 m high with subdued relief. Between 1320 and 1500 m depth, it is surmounted by two narrow ridges up to 150 m high and 2–3 km long which are parallel to the main ridge. Adjacent to, and down slope from, these ridges is a terrain extending for 11 km between the 1500 to 2000 m isobaths which consists of irregular mounds up to 120 m high and with lobate margins. The area is interpreted as a series of lavas fed from fissures along the ridges. A similar, but wider terrain extending 18 km between the 1000 and 2600 m isobaths occurs on SW-trending Ridge S5. This has mounds typically 100–120 m high with irregular, lobate margins, and occurs down slope of two 120–150 m high ridges. Within this area at 57°53.2′S 26°47.6′W there is a well defined circular, 0.8 km diameter, 150 m deep crater surmounting a 2.4 diameter, 300 m high cone that rises from the 2250 m isobath to 1949 m at the crater rim. This area is also interpreted as a as a lava field fed from fissures along the ridges. The crater is likely to be a volcanic collapse 'pit' crater formed by magma withdrawal.

Embayments SE1 and SE2, 7.0 and 8.2 km across respectively, have steep north walls, and are interpreted as collapse scars, although

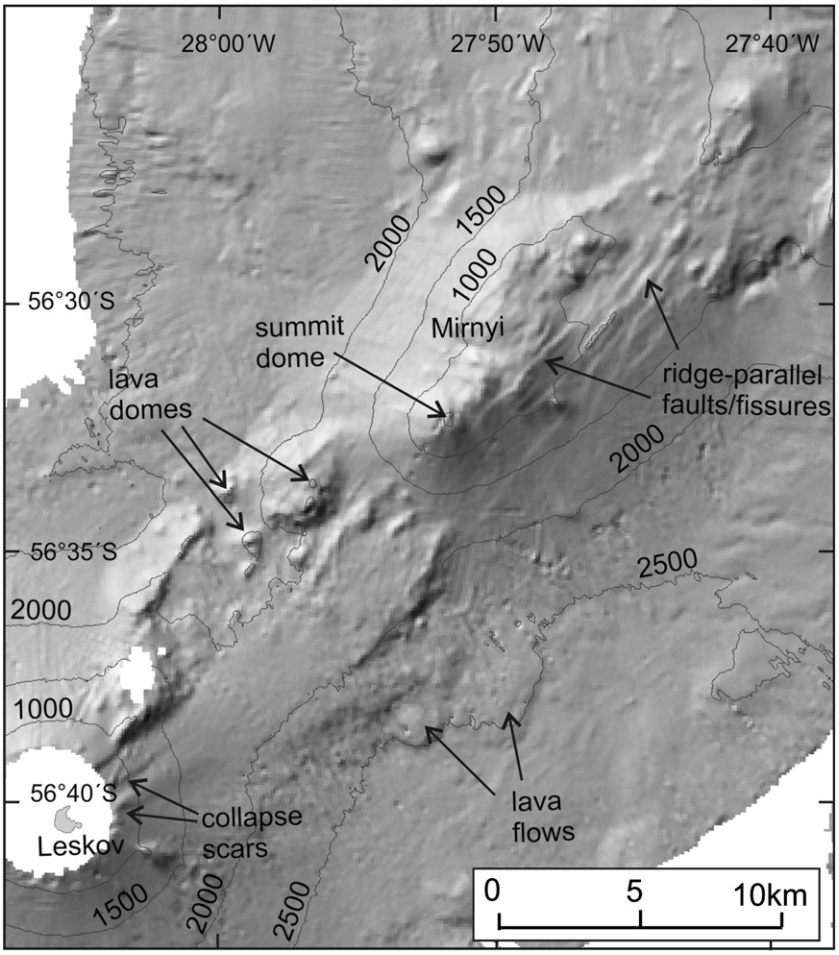

Fig. 6. Hillshade image of part of Leskov seamount chain from Mirnyi to Leskov. Isobath interval 500 m.

modified by constructional ridge S5 in the case of SE1 and partially filled by a debris fan sourced near Harper Bank in the case of SE2. Ridge S6 is interpreted as an erosional remnant of Saunders Bank, similar to S1 to S3.

The large seamounts around the Saunders were newly discovered during the survey. The north Saunders seamount chain comprises Minke, Orca and Humpback and West Minke, the last being 14 km N of the chain axis (Fig. 7A). Conical Orca has an approximately flat top 2.9 km across shallower than 420 m and with a minimum depth of 344 m. There is a subdued central depression some 30 m deep and 1.5 km across. This is interpreted as a summit crater. The upper crater walls are unusually rounded and smoothed, and it is likely that the upper parts of the cone have been modified by iceberg scouring. Humpback has a rugged axial spine that extends 3.7 km at less than 250 m depth, with a summit at 75 m. There is no topographic evidence of a shelf cut into the summit, implying that the summit is more recent than the Last Glacial Maximum. The south Saunders seamount chain consists of Fin and near-conical Southern Right. Fin has a minor, satellite seamount rising to 733 m depth on its SW flank, along the trend of the seamount chain. Fin rises to 246 m depth, and has an approximately flat summit 0.5 km across shallower than 259 m, and Southern Right has an approximately flat top 0.6 km across less than 400 m depth. The flattened summits are interpreted to be a result of erosion by iceberg scour. All the seamounts, apart from the satellite seamount on Fin, have scars originating near their summits that extend to their basal slopes. All of the scars are on the western sides of seamounts, apart from Humpback, which has several radiating from its summit. The scars are broad, linear depressions, generally 35–80 m deep and 0.6–1.0 km wide. Most are 3.1–5.8 km long and the largest is a 10.3 km long, 1.3 km wide and up to 90 m deep scar on the west slope of Fin.

On the west, south and particularly east flanks of the Saunders edifice are regular wave-like forms (picked out by slope analysis; Supplementary Material S3) that generally parallel isobaths and are interpreted as sediment waves. Close to Saunders, they occupy lower topography, notably either side of S3, and in embayments SE1 and SE2. They continue down slope forming fan-like arrays and extend up to 40 km from the shallow shelf.

3.4. Montagu

Montagu is revealed as a simple cone-like volcano with few topographic complications (Fig. 8A). The island is about 12 km across (Patrick et al. (2005) noted that the map in Holdgate and Baker (1979) inaccurately suggests a larger size). Most of the island is occupied by an ice dome that reaches an altitude of 1372 m at Mount Belinda, a small summit volcanic cone (Fig. 8B). Much of the coast of the island is formed by ice cliffs, although the north coast is dominated by rock cliffs up to 600 m high; similar but lower rock cliffs occur along the west coast. The SE end of the island is formed by a steep-sided, 900 m high satellite cone, Mount Oceanite. The east-facing flank of this cone forms the headwall of a small collapse scar (Fig. 8C) which is not seen to continue offshore in the multibeam bathymetry. Patrick et al. (2005) interpreted the ice dome on Montagu Island as a largely ice-filled caldera some 6 km across occupying the central part of the island (Fig. 8B). The most recent eruption, largely observed through visible-light, infra-red and radar satellite data with infrequent observations from ships and one landing on the

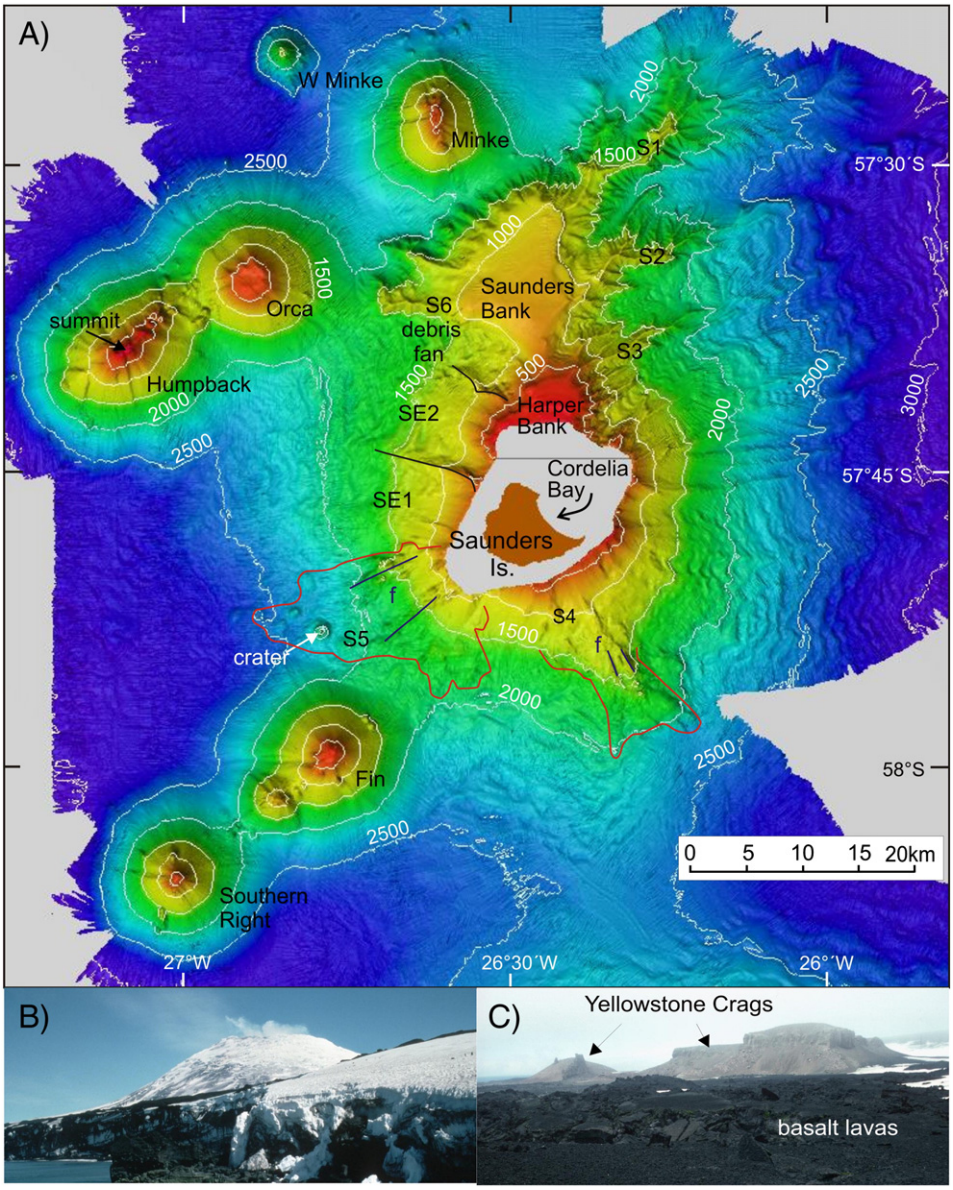

Fig. 7. Images of the Saunders edifice. A. Multibeam bathymetric map of the area around Saunders Island. Isobath interval 500 m. Feature names apart from Saunders Island and Cordelia Bay are unofficial. Positive features S1-S6 and embayments SE1 and SE2 are described in the text. Black solid lines indicate interpreted margins of collapse scars. Red lines are interpreted lava flow fronts, with associated fissures (f) indicated. B. Photograph of Mount Michael from Cordelia Bay with low coastal cliffs in the foreground. C. Photograph of former sea stacks of Yellowstone Crags surrounded by recent basalt lavas.

island during the activity, lasted from late 2001 until late 2007 (Patrick et al., 2005; Patrick and Smellie, 2013). The eruption originated within the caldera and consisted of small-scale explosive activity at the summit and effusion of a number of lava flows one of which reached the sea and produced a small lava delta on the north coast of the island. A larger, older lava delta forms the NW point of the island.

The area close to the islands with depths less than 500 m depth was very incompletely surveyed due to grounded icebergs. Sea stacks rise from the shallow shelf within about 1 km from the island along its north and west coasts, the highest being Longlow Rock to the west of the island and which is about 30 m high (Holdgate and Baker, 1979). These suggest an extensive shallow shelf. The largest area of mapped shelf is Longlow Bank, west of the island, which covers a 6.0 by 4.8 km area at depths of less than 600 m, rising to a plateau at around 380–250 m depth toward the island.

Multibeam data show that the base of the Montagu volcano rises from 3000 m in the west, and about 2000 m in the east where its lower slopes overlie a basement high from which volcanic rocks K–Ar dated at ca. 30 Ma were dredged (Barker, 1995). The edifice is roughly circular in plan with a diameter of 62 km at the 2000 m isobath. Ridge M1 is asymmetrical, with its west-facing (18–34°) steeper than its east-facing (12–17°) slope. From ridge M1 to ridge M2, a series of radial ridges and valleys occupy the NE of the edifice above 1750 m depth. The valleys are 340–425 m deeper than the ridges on either side, and up to 4.4 km wide. Ridge M2 is also asymmetrical, with its north-facing (17–24°) steeper than its south-facing (10–15°) slope. The asymmetrical ridges M1 and M2 may be side walls of landslide scars to their west and north respectively, and the valleys between M1 and M2 may be smaller landslide scars modified as sediment chutes. M3 is a heavily sedimented segment of the edifice that slopes gently (generally <9°) south to a col at 1580 m between the Montagu and Bristol edifices. From M3 to Longlow Bank, there are further ridges and irregular valleys which may be landslide scars. Longlow Bank surmounts a prominent ridge 9 km across at the 1250 m isobath that extends west from the main Montagu edifice. It has relatively steep slopes, some 16–24° along the 1000 m isobath,

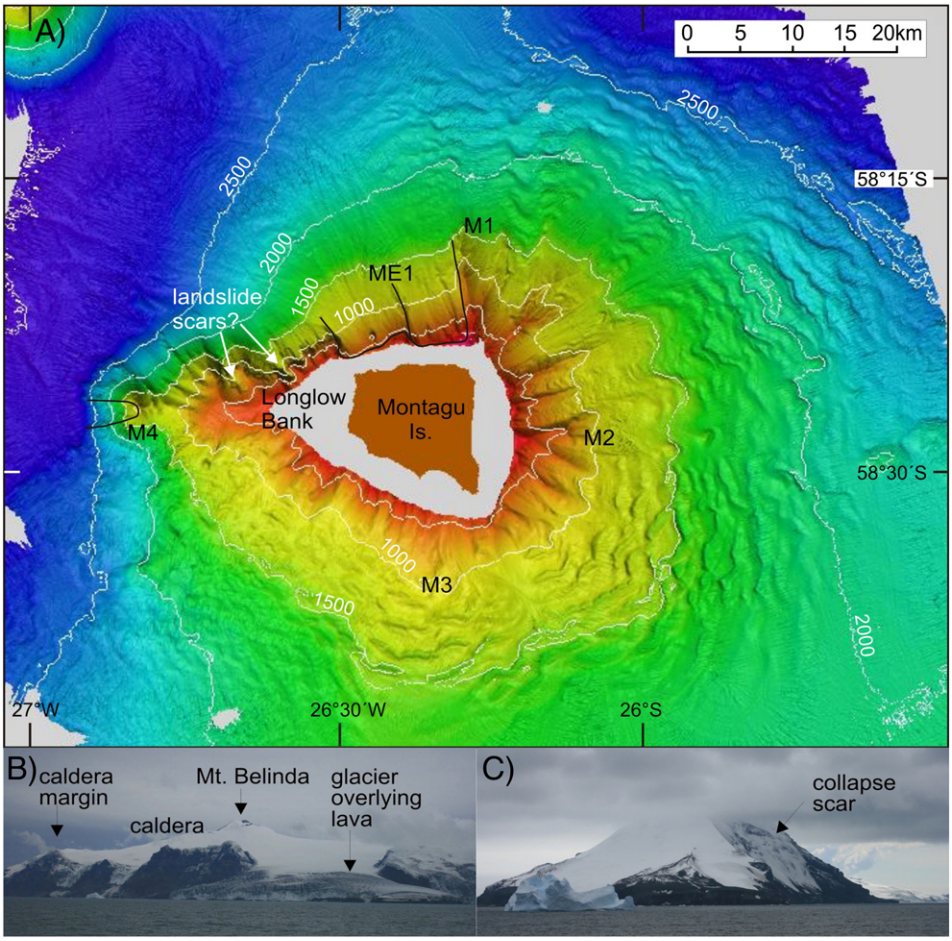

Fig. 8. Images of the Montagu edifice. A. Multibeam bathymetric map of the area around Montagu Island. Isobath interval 500 m. Longlow Bank is an unofficial name. Positive features M1-M4 and embayment ME1 are described in the text. Black solid lines indicate interpreted margins of collapse scars. B. Photograph taken from NW of Montagu Island showing high coastal cliffs, the caldera margin and Mount Berlinda. C. Photograph of Mount Oceanite taken from the south showing small collapse scar.

and appears not to have been strongly modified by lateral collapse, although on its north side there are two small embayments, 1.3 and 2.0 km across respectively, which may represent landslide scars. It is interpreted to represent a separate volcanic centre, west of the main Montagu volcano. Conical seamount M4 rises over 1500 m on its west flank from about the 2500 m to 984 m isobaths. Slopes away from its summit to the north, west and south are mostly 19–23° above 2000 m depth and 14–17° on lower slopes below 2000 m. On its western flank is a 1.4 km wide embayment that extends 4 km from the summit to 2300 m depth. This is tentatively interpreted as a landside scar. Embayment ME1 is 13.1 km across and extends from the shallow shelf at about 100 m in the east (and 400 m in the east limited by the multibeam coverage) to about 1500 m depth. It has inward facing side walls 490 m and 350 m high respectively forming its NE and SW margins. It has a deeper subsection 6.1 km across forming its NW sector suggesting that ME1 was produced by at least two successive collapse events.

Sediment waves occupying the north, east and south flanks of Montagu (Fig. 8A) are among the largest in the area, typically having wavelengths of 1.4 to 3.7 km and amplitudes of 85–200 m. They extend from 700 m to at least 2800 m depth, 42 km from the shelf.

3.5. Bristol

Bristol Island is approximately square in plan, with a maximum dimension of 11 km in the east–west direction (Patrick and Smellie, 2013). It is almost entirely ice covered, and most of the coast consists of ice cliffs. The summit is at Mount Darnley, 1097 m high, south of its centre. The island is almost entirely inaccessible, has only been visited at a few points, and is geologically poorly known. A well-observed eruption occurred at the summit area in 1956 and was characterised by strombolian activity (Holdgate, 1963). Holdgate and Baker (1979) described steaming pits and fissures in the glacier ice cover observed in 1962–3.

The shallow shelf around the island was poorly surveyed. Depths mostly less than 180 m depth were surveyed on all sides of the island (Fig. 9A), and shallow shelf with depths of 118 m and 126 m was encountered south and north of the island respectively. A prominent part of the shelf west of the island forms Freezland Bank which is 6 km across and mostly 145–205 m deep, from which rise a group of prominent sea stacks, Grindle Rock, Wilson Rock and the largest, Freezland Rock, which is 305 m high (Holdgate and Baker, 1979). The presence of these sea stacks suggests extensive shallow shelf west of the island.

The multibeam data show that the Bristol edifice has a relatively simple cone shape, 90 km across at the 2500 m isobath (Fig. 9A). The NW sector of the submarine volcano (Ridge B1) has relatively gentle slopes, generally <8°, and is unaffected by large collapse structures or constructional ridges. To the SE, between B1 and B2, the upper submarine slopes are cut between approximately 250 and 750 m by embayments 2.2–3.5 km across leading down to chute-like valleys. Ridge B2 extends 11.9 km from to shallow shelf to the 1500 m isobath. It has a summit at 763 m below sea level, 4.8 km from the shelf edge. It is asymmetrical, with a steep (15–22°), 530 m high west-facing flank, that forms the SE margin of embayment BE1, interpreted as a collapse scar.

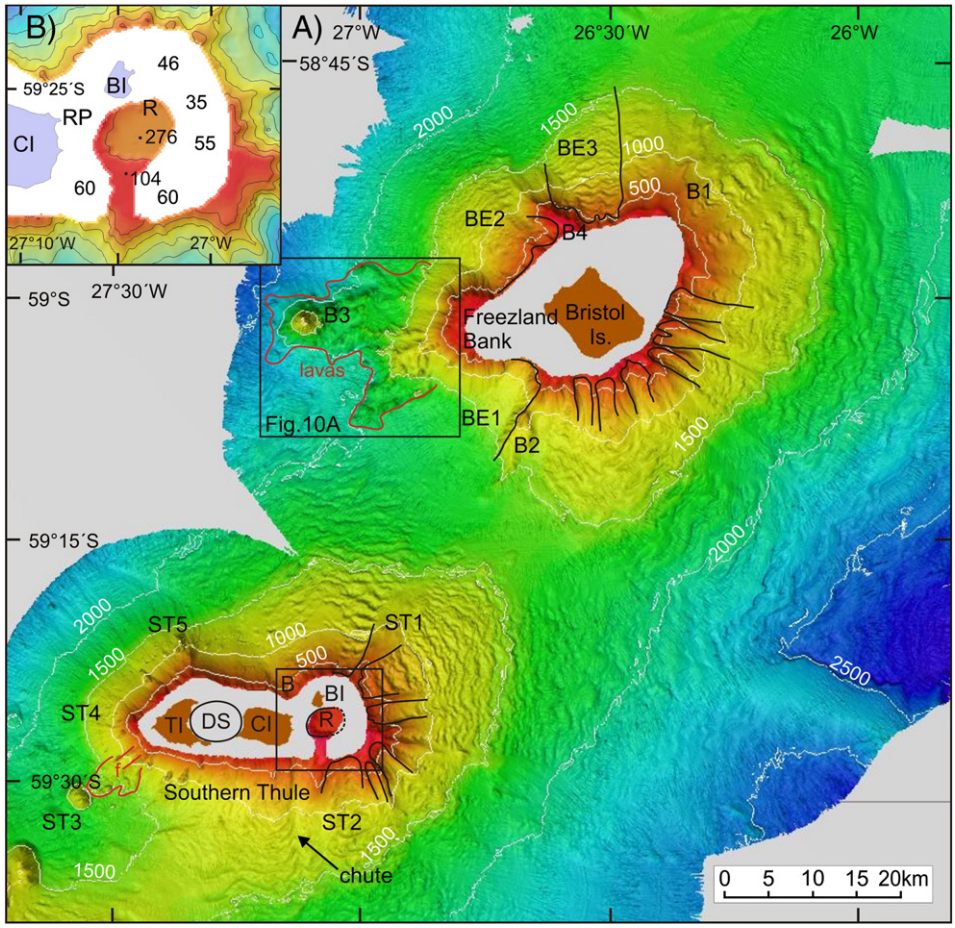

Fig. 9. A. Multibeam bathymetric map of the area around Bristol Island and the Southern Thule island group. Isobath interval 500 m. Freezland Bank is an unofficial name. Positive features B1-B4 and ST1-ST5 and embayments BE1-BE3 are described in the text. Black solid lines indicate interpreted margins of collapse scars. Red line indicates interpreted lava flow fronts. B. Bathymetric map of the eastern part of the southern Thule volcanic edifice, showing position of the inferred Resolution Caldera. Isobath interval 100 m. Depths indicated by points are from the multibeam data, other points are from the Admiralty Chart (Hydrographic Office, 2003). TI, Thule Island; DS, Douglas Strait Caldera; CI, Cook Island; R, Resolution Caldera, RP, Resolution Point; BI, Bellingshausen Island.

Freezland Bank is shown as the summit of a roughly circular construct joined to the main part of the Bristol edifice that is 12 km across at the 1000 m isobath. Its upper flanks around 500 m slope are up to 22°, and are 15–20° at 1000 m depth. Its slopes are unaffected by large collapse scars. It is interpreted as a volcanic centre, now mostly eroded to below sea level, partly occupying the BE1 collapse scar, and also the BE2 embayment to the north. The sea stacks on Freezland Bank are eroded remnants of volcanic constructs, and Freezland Rock yielded the oldest K–Ar age (3.1 Ma) obtained from the South Sandwich Islands by Baker et al. (1977). Holdgate and Baker (1979) suggested that that the sea stacks are remnants of a volcanic centre that preceded much of the volcanism on Bristol Island. The bathymetry indicates that a separate volcanic centre forming Freezland Bank may have existed, but that it post-dates embayments BE1 and BE2, and therefore most of the Bristol edifice. Conical seamount B3 is over 1000 m high, rising to 973 m depth from a base of approximately 2000 m, with slopes of 19–33° (Figs 9A, 10A). A terrain between the lower slopes of the Freezland volcano and seamount B3, and also extending west of B3, consists of knolls and terraces generally stepping down away from the Freezland volcano. The terraces are generally 130–250 m high and lobate in plan view. The terrain extends 18 km in a north–south direction and 17 km east–west (Fig. 10A). The terrain is interpreted as multiple lava flows, apparently sourced from the basal area of B3 and Freezland volcano. At the likely source area of the lavas at 750–1500 m on the lower slope of Freezland volcano there are three 3.5–5.2 long, radial ridges 80–150 m high which are interpreted as eruptive fissures. It is uncertain why this recent volcanism occurred on the lower flanks of Freezland volcano when its summit area appears to be extinct. NW-facing, 10.3 km wide embayment BE2 cuts the upper slopes of the edifice to shallower than 250 m in its NE part, but the multibeam coverage did not extend onto the shallow shelf in this segment. Its NE side wall on the south side of B4 is 480 m high and slopes at 14–23° into the embayment. It is interpreted as a landslide scar, whose SW wall is covered by younger deposits of Freezland volcano. Embayment BE3 cuts into the upper slopes of the edifice to about 350 m, where its upper limit was not covered by the multibeam data. It is 5.6 km wide in its upper part, and widens down-slope to the north. The NE-facing slope of B4, which forms its SW wall, is 450 m high and slopes at 17–22° toward the embayment. The east wall of the embayment is a 100 m high, east facing slope that extends 14 km to the north. BE3 is also interpreted as a collapse scar.

Sediment waves occur on most flanks of the Bristol edifice. On the eastern flanks, between ridges B1 and B2, the waves are relatively large, typically with wavelengths of 1.1–2.8 km and amplitudes of 38–87 m, comparable to those on the east flank of Montagu. These sediment wave fields extend from 820 m depth to the limit of the survey area at over 2500 m, some 43 km from the shallow shelf.

3.6. Southern Thule

Southern Thule is relatively well-described in the literature (Holdgate and Baker, 1979; Smellie et al., 1998; Leat et al., 2003; Allen and Smellie, 2008; Patrick and Smellie, 2013). It consists of three main islands. Cook Island, the largest of the group, is 6 km

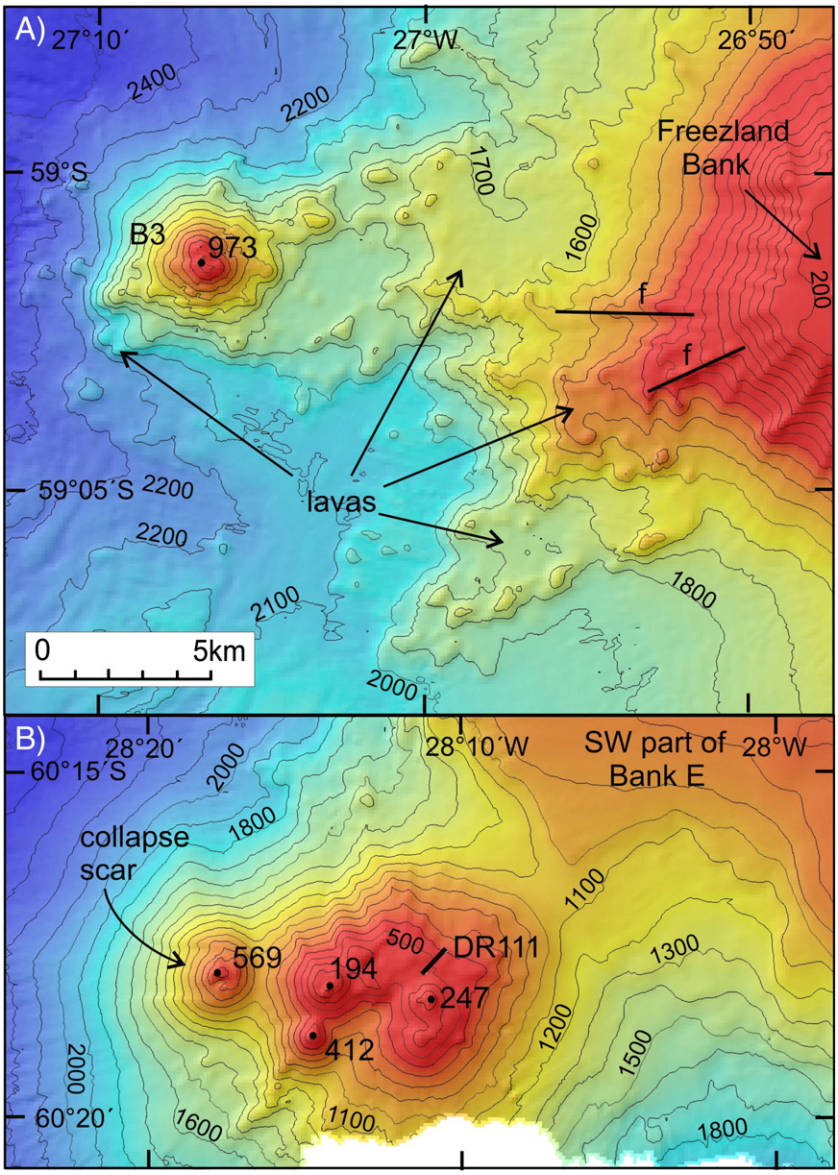

Fig. 10. Detailed bathymetric images. A. Terrain interpreted as recent sea floor volcanism west of Bristol Island. Terraces are interpreted as lava flows, fed by possible fissures (f). B. Nelson Seamounts. DR111 is a dredge site on Nelson Seamounts that yielded dacites (Leat et al., 2004). Contour interval for both images is 100 m. The images have the same horizontal scale, but not the same colour scales. Depths indicated by points are from the multibeam data.

across and 1067 m high and is ice-covered. Thule Island, in the west of the group, is also ice covered, 5.4 km across and 725 m high. Bellingshausen Island, 1.7 km across and 253 m high, is a largely ice-free, recently active volcanic cone, and is persistently fumarolically active. The new multibeam data show that the submarine part of Southern Thule forms an east–west elongated edifice, 63 km across at the 2000 isobath (Fig. 9A). There is an east–west contrast in bathymetric features. The eastern part of the edifice has relatively gentle slopes interrupted by ridges. Slopes on the west part of the edifice are steeper, with less pronounced ridges.

Structurally, the island group is defined by an east–west line of three calderas. The most westerly caldera underlies the summit area of the island of Thule, is ca. 1.7 km across (Smellie et al., 1998; Patrick and Smellie, 2013) and visible in satellite images and aerial photographs. It is ice-filled and the rim is apparently not greatly modified by glacial erosion, suggesting that it is morphologically young. It is probably within this caldera that the partly water-filled crater present in 1962 (Holdgate, 1963), and observed as a 'dimple' thereafter (Allen and Smellie, 2008) is situated. The central caldera occupies Douglas Strait between Cook and Thule islands. The 1997 and 2006 echo sounder surveys show that the 5.1 by 4.0 km caldera is steep-walled, and has a relatively flat floor ca. 620 m below sea level (Smellie et al., 1998; Allen and Smellie, 2008).

A third inferred caldera, Resolution Caldera, was mapped to the east of Cook Island. This is shown on the Admiralty Chart (Hydrographic Office, 2003) as a circular submarine depression centred to the SSE of Bellingshausen Island and SE of Resolution Point, Cook Island. During cruise JR206, the ship was navigated over the depression by crossing the southern caldera rim. The notably flat floor of the depression has a maximum depth of 276 m below sea level and its margins were mapped to the west and south, using the multibeam echo sounder, where steep walls are observed to rise to <150 m depth. To the east, the Admiralty Chart shows reefs rising to as shallow as 35 m below sea level (Fig. 9B). The structure is therefore unlikely to be an east-facing landslide scar. To the north, Bellingshausen Island is situated on the rim of the depression. The depression therefore appears to be roughly circular in plan, some 3–4 km across with a typical depth below rim height of 200 m, and it is interpreted as a caldera. There

are few wide shallow shelves around Southern Thule. The widest is around Resolution Caldera, where depths of 130–180 m extend 4.3 km SE from the caldera rim.

The NE ridge of the Southern Thule edifice, ST1, has a 300 m high west-facing 17–23° slope and a 170 m high 11–21° SE-facing slope (Fig. 9A). Several 80–250 m high ridges separated by valleys dominate the eastern slopes of the edifice above 1000 m between ST1 and ST2. The valleys have steep-inward facing head and side walls, are 1.6–5.7 km across, and have head walls which cut the shallow shelf at less than 250 m. They may be modified landslide scars. West of ST2, there is a prominent 100 m deep, 2–3 km wide chute (Fig. 9A) and then a relatively gentle south-facing slope that steepens to the west. Conical seamount ST3 is 3.5 km across and rises to 1189 m from a base at 1650 m depth. NE of ST3, there is a terrain at about 1500 m depth consisting of approximately conical mounds 80–150 m high and up to 1 km across associated with terraces. These features are tentatively interpreted as constructional volcanic ridges and lava flows or domes (Fig. 9A). ST4 and ST5 are constructs with no obvious modification by collapse or constructional volcanism. Between ST5 and ST1, the slope is to the north, becoming less steep to the east, where it is interpreted to have been modified by a debris fan sourced near Bellingshausen Island. The steep west-facing slope of ST1 is interpreted as the side wall of a collapse scar, now largely filled by the fan.

There is an east–west contrast in distribution of sediment waves around the Southern Thule group. To the west, around the island of Thule, the submarine slopes are mostly smooth, with few sediment waves. To the east, there are well-developed sediment wave fields that can be traced 29–36 km to the north, east and south.

3.7. Adventure

Adventure volcano was discovered during the 2010 survey (Leat et al., 2010b). It is the east part of an east–west elongated group of volcanic edifices which includes Kemp Seamount (Barker, 1995) Kemp Caldera (discovered during cruise JR224, Supplementary Material S1), seamounts VB1 and VB2, which rise to 708 m and 805 m depth respectively, and smaller associated seamounts that together form the positive topographic feature Vysokaya Bank (Fig. 11). The whole edifice is interpreted as the southernmost volcanic complex of the volcanic front. Adventure volcano is some 68 km across above the 2000 m isobath, and is roughly conical above the 1250 m isobath (Fig. 12). Adventure Caldera is centrally located on the volcanic cone and slightly elliptical with a 6.5 km NE–SW major axis and 5.2 km minor axis (Fig. 12). The caldera floor is approximately flat, 784–793 m below sea level in its west and central areas, and rises to 750 m depth in the east. On the southern part of the caldera floor, there is a cluster of about six 0.6–1 km diameter mounds with subdued slopes that rise 100–230 m above the caldera floor. These are interpreted as post-caldera lava domes, with some of the feeders possibly occupying the caldera fault.

The shallowest part of the caldera rim is on plateau AD1, which is 1.6 km across and mostly 200–260 m below sea level, peaking at 168 m. A distinct 0.63 km diameter crater which is 170 m deeper than its rim is situated near the centre of the plateau. Embayment ADE1 has a semi-circular headwall 2.6 km across, steep, inward facing walls up to 150 m high, a gently-sloping floor and is interpreted as a landslide scar. Plateau AD2 rises to 242 m below sea level at the caldera rim. A wide, flat topped ridge mostly at 900–1040 m depth continues to the NE for 13 km. At its NE end, its margins are cut by 300–400 m high embayments, and there are no lobate or conical constructs that would suggest recent eruptions. This lower part of the ridge is morphologically similar to Saunders Bank and is tentatively interpreted as a subsided bank. Ridge AD3 rises to 211 m below sea level, and appears to be an unmodified part of the caldera rim. To the southeast, embayment ADE2 is 2.4 km across, has a semicircular headwall, steep, inward-facing slopes 140–160 m high on to the east and 50–92 high to the west, and is interpreted as another landslide scar.

To the west, flat-topped plateau AD4 forms a separate part of the edifice, rising to 115 m below sea level. It is 4.4 km across and almost surrounded by 400–600 m high 20–30° slopes. These slopes are locally scalloped, and a distinct embayment, ADE3, forms its SW slope. This embayment is 2.3 km across, has steep inward-facing slopes some 140 m high, has a central ridge and a smooth floor, and is interpreted as a landslide scar. No constructs interpreted as recent lavas or cones are present on AD4. It is interpreted as a shallow shelf remnant representing a now extinct volcanic edifice that was eroded at, or never rose above, sea level, and whose flanks were extensively modified by landsliding.

Well-formed fans of wave-like structures having typical wavelengths of 1.0–2.3 km, wave heights of 50–90 m and interpreted as sediment waves radiate to the north, east and SW of Adventure volcano. The northern fan extends 30 km from the upper cone with no apparent source focus, although one regular group of waves seem to originate in ADE1. The east-directed sediment wave field has a source focus on the east-facing slopes of AD2 and AD3. The SW field can be traced for 37 km and covers the rifted margin of the back-arc basin (Fig. 11).

3.8. Bank E

Bank E is situated south of Vysokaya Bank and extends from a west-facing escarpment south of 59°52 S to the southern boundary of the Sandwich plate at the Sandwich–Antarctic plate boundary transform fault. Previously assigned as Area E (Hamilton, 1989), it forms flat topography sloping gently at 1–3° to the ENE, and rises to 645 m (Fig. 11). The escarpment forming the west edge of the Bank is made by a series of faults stepping down to the west a total of ca 800 m to the floor of segment E9 of the back-arc spreading centre. There is no evidence of deformation cutting sediments at fault bases, suggesting that they are now inactive. To the east, the transition to the fore-arc is marked by a nearly flat, sediment-covered surface. Interpretation of multichannel seismic reflection data indicates that Bank E is underlain by some 3 km of east-dipping sedimentary sequences (Hamilton, 1989). The underlying crystalline basement has not been sampled. Nevertheless, its flat, eroded topography suggests that it is a fragment of crust that predates the current South Sandwich arc, and was rifted along its current eastern boundary (and tilted) during opening of back-arc segment E9.

3.9. Nelson Seamounts

Nelson Seamounts form a cluster to the SE of Bank E, and are the southernmost volcanoes on the Sandwich plate (Fig. 11). Geophysical investigations in the 1970s indicated a single seamount in this position, called Nelson Seamount (Barker, 1995). The new data show a seamount cluster some 13 km across and rising from ca. 1100 m in the north and east where they are adjacent to Bank E, and some 2000 m from the ocean floor to the west (Fig. 10B). The largest seamounts form an alignment trending 100°, approximately east–west. The east seamount of the group rises to 569 m and has a 1.7 m wide west-directed landslide scar on its western flank. The central and eastern seamounts rise to 194 and 247 m respectively and coalesce below approximately 500 m. The north slope of the east seamount was dredged in 1985 by RRS *Discovery* (Barker, 1995) yielding dacites (Leat et al., 2004).

4. Discussion

The new data can be used to comment on tectonic structure and the processes that formed the volcanoes in the volcanic arc. All the large volcanoes of the volcanic front arc show bathymetric evidence for multiple periods of growth and mass wasting.

4.1. Volcanic development and structure of the arc

The main volcanic edifices form a well-defined linear, convex-east, array which clearly defines a volcanic front along the line of the seven

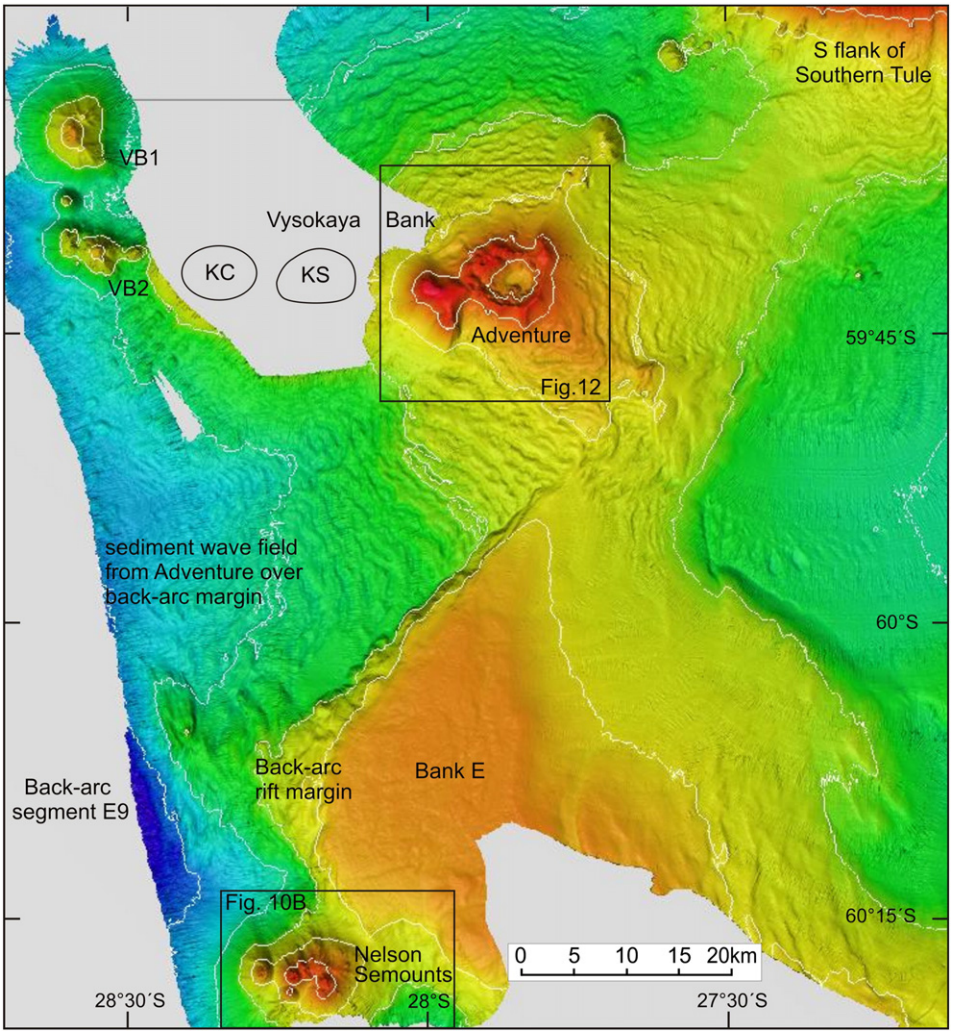

Fig. 11. Multibeam bathymetric map of Vysokaya Bank, Adventure volcano, Bank E and Nelson Seamounts. KC, Kemp Caldera; KS, Kemp Seamount (Barker, 1995) surveyed on cruise JR224 (Supplementary Material S1).

large volcanoes from Zavodovski to Adventure. The simple structure is consistent with the relatively young age (ca. 10 Ma) of the arc compared to the more complex, longer-lived Tonga–Kermadec, Mariana and Izu–Bonin intra-oceanic arcs (Ishizuka et al., 2003; Graham et al., 2008b; Oakley et al., 2009; Wysoczanski et al., 2010). Most of the volcanic front volcanoes have summits 3.0–3.5 km above base levels, which are deeper in the north (2500–3000 m) than in the south (2000–2500 m). Volumes above the same base level are larger in the south than the north (Fig. 2). The southernmost volcanic front volcano, Adventure is somewhat smaller than the other southern volcanoes, rising to only 2.0 km above base level. There are three cross-cutting, rear-arc seamount chains. The northernmost volcanism in the arc consists of a broadly east–west trending group of polygenetic seamounts situated around Nimrod bank. The seamounts overlie a major east–west tear in the subducting plate (Forsyth, 1975), and it is possible that this tear influences the position of the line of seamounts, perhaps by enhanced fluid flow from the subducting plate edge (Leat et al., 2007). In the south, Nelson Seamounts are situated south of the termination of the concave volcanic front, close to the transform boundary of the Sandwich plate, and thus overlie the subducting plate edge. Sr–Nd isotope relationships in the Nelson Seamount dacites suggest a high sediment input, anomalous in relation to volcanic front composition, interpreted to be related to enhanced sediment melting at the subducting plate edge (Leat et al., 2004).

Evidence for faulting is very localised in the arc. Within the part of the arc occupied by the main volcanic front volcanoes, there is no topographic evidence of faulting, except on Mirnyi Seamount. Otherwise, faults are only evident close to the north and south boundaries of the Sandwich plate where they appear to be components of deformation along the plate edges. North–south trending faults down-faulting Bank E toward the back-arc spreading centre are interpreted to result from rifting to form the southern part of the back-arc basin. The pre-arc and pre-back-arc basement that was rifted is clearly represented by peneplained and tilted Bank E. Similar basement may be present in a fore-arc high 75 km SE of Montagu Island at 58°41′S, 25°3′W where volcanic rocks were dredged and K–Ar dated at 28.5–32.8 Ma (Barker, 1995). These may represent parts of a remnant arc that pre-dates the current arc Barker (1995). Larter et al. (2003) suggested that fore-arc basement indentified in seismic data 70 km ESE of Cook Island represents the same remnant arc. If these outcrops are parts of the same basement, remnant arc crust likely underlies a 240 × 70 km area of the Sandwich plate from Montagu to the southern plate boundary, perhaps accounting for the higher volcano base level in the south. In contrast, north of Montagu, where volcano base level is deeper, no such basement crust to the arc has been imaged or identified, and magnetic data suggest oceanic crust formed at the East Scotia Ridge continues east and underlies the current arc (Larter et al., 2003).

4.1.1. Seamount cross-chaINS and rear-arc volcanism

The three cross-cutting seamount chains form significant structures in the northern sector of the arc from Zavodovski to south of Saunders

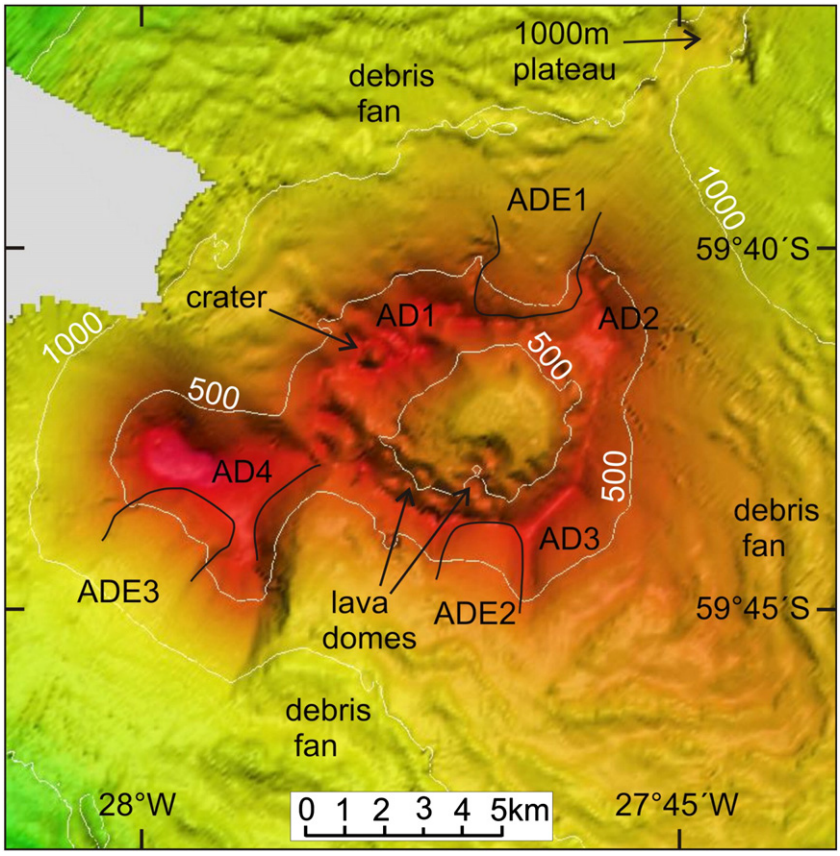

Fig. 12. Multibeam bathymetric map of Adventure volcano showing the prominent caldera. Isobath interval 500 m. Positive features AD1-AD4 and embayments ADE1-ADE3 are described in the text. Black solid lines indicate interpreted margins of collapse scars.

(Fig. 2 and Table 1). The seamount chains are situated entirely to the west of the volcanic front, in a rear-arc position extending 38–60 km toward the back-arc. Our use of the term rear-arc follows that of Taylor and Nesbitt (1998) and Stern et al. (2006), referring to magmatism distinctly farther from the trench than the volcanic front, but also distinct from more distal back-arc basin magmatism. Several of the seamounts in the chains rise more than 2.0 km above base level with volumes over 140 km^3 (Table 1). All three chains form parallel trends at N 30–43°E. Because of the curvature of the arc, these intersect the volcanic front at 60–65° at Saunders, and at 78° at Zavodovski. This suggests that the seamount chains are tectonically controlled by parallel NE–SW fractures of the Sandwich plate rather than by boundary forces at the subducting margin. The origin of the NE–SW fractures of the plate is uncertain. Segments of the back-arc spreading centre are separated by non-transform offsets and magnetic fabric trends north–south, so NE–SW structure is not evident in the back-arc ocean crust (Larter et al., 2003). NE–SW trending faults cut the northern part of the Sandwich plate (Fig. 3), which are possibly a result of plate boundary forces and the seamount trends may be controlled by the same stresses.

The cross-cutting South Sandwich seamount chains are comparable to en echelon seamount chains between 30° and 32.5°N in the Izu–Bonin arc which extend similar distances (some 40–70 km from the intra-arc rift zone) toward the back-arc basin, intersect the arc trend at similar angles (approximately 70°), and have similar volumes (typically 50–100 km^3 for individual seamounts) (Ishizuka et al., 2003; Machida et al., 2008). Seamount chains with similar dimensions and cross-cutting relationships also extend from the volcanic arc into the rear-arc in the Northern Seamount Province of the Mariana arc (Stern et al., 1993). Ar–Ar dating of the Izu–Bonin back-arc seamounts indicates that they are locally as old as 17 Ma but mostly erupted during the period 10–3 Ma with age progression of magmatism along the

Table 1
Summary of features of seamounts in cross-cutting seamount chains.

Seamount	Summit latitude	Summit longitude	Basal contour (m)	Shallowest point below s.l. (m)	Height (m)	Basal diameter (km)	Estimated volume (km^3)[1]	Flank slopes (°)[2]	Features
Mirnyi	56°32.2′S	27°51.8′W	2000	445	1555	13	118	15–27	Elongate along chain axis
Leskov Island	56°40.1	28°06′W	2500	+190[3]	2690	19.5	234	14–22	Emergent
Vostok	56°43.0′S	28°14.2′W	2500	1139	1361	13	31	13–22	Landside scars on SW flank
West Minkie	57°24.4′S	26°51.4′W	2500	1429	1071	5.5	8	19–26	14 km N of chain axis
Minkie	57°27.6′S	26°37.2 W	2000	364	1636	12.7	59	16–24	Slightly elongate on N–S trend
Orca	57°35.7′S	26°53.9 W	2250	344	1879	20	169	11–22	Probable summit crater
Humpback	57°39.2 S	27°05.2 W	2500	75	2425	22	234	18–30	Elongate along chain axis
Fin	57°59.1′S	26°46.2 W	2250	246	2004	15	148	16–25	Satellite seamount to SW
Southern Right	58°05.4′S	27°00.9′W	2500	386	2114	16	112	18–25	Conical

1, Calculated using ARC GIS function; 2, slopes are those on upper flanks at 250–1000 below summits; 3, height above s.l. from Holdgate and Baker (1979).

chains toward the volcanic front (Ishizuka et al., 2003). Such long-lived magmatism along narrow loci suggests lithospheric structural control. Cross-arc chains in the Kermadec arc such as Rumble V Ridge are likely to have a similar origin (Wright et al., 1996; Todd et al., 2010; Wysoczanski et al., 2010). However, there is thought to be no age progression along Rumble V Ridge in the Kermadec arc, with recently erupted lava observed along its length, and Wysoczanski et al. (2010) concluded that the ridge represents the surface expression of a zone of dyke intrusion in the crust. In the case of the South Sandwich seamount chains, the large size of the seamounts indicates prolonged magmatism controlled by lithosphere structure, as proposed for the Izu–Bonin arc.

Evidence for minor, relatively recent volcanism is a feature of west-facing, rear-arc flanks of all the large volcanoes of the volcanic front. Examples include the seamounts and, in some cases, interpreted lava fields west of Montagu, Bristol and Southern Thule, and seamounts and monogenetic volcanoes west of Visokoi and Candlemas (Leat et al., 2010a). At Bristol, such volcanism is well developed and extends 14 km west of the main volcano flank (Fig. 10A). In most other cases, the volcanism extends no farther than 7.5 km west the main volcanoes. Similar flank volcanism toward the rear-arc in the Izu–Bonin arc is interpreted to result from lateral flow of magma in dykes away from the central volcanoes (Kaneko et al., 2005; Ishizuka et al., 2008).

4.2. Shallow shelves

Shallow shelves are present around all of the emergent volcanoes. The presence of sea stacks, reefs and floating and grounded icebergs prevented most of the shallow areas close to the islands being surveyed. Nevertheless, where parts have been surveyed, they are relatively flat and generally have depths of less than 250 m. Extensive areas are shallower than this. Cordelia Bay NE of Saunders Island is about 30–50 m deep, and parts of shelves at Bristol and Southern Thule are 120–130 m below sea level. Most of the shallow shelves are characterised by numerous sea stacks and submerged rocks which cause breaking waves. Such sea stacks occur on Freezland Bank, west of Bristol, Longlow Bank, west of Montagu and Blackstone Plain, in the north of Saunders Island, where previously-formed sea stacks are now surrounded by subaerial lavas. These features suggest extensive shallow areas. Leat et al. (2010a) noted the presence of similar shallow shelves around Zavodovski, Visokoi and Candlemas in the northern part of the arc, and concluded that they were the products of erosion of wave-cut platforms during low sea level stands, flowing similar interpretations of shallow shelves around volcanic islands in the Lesser Antilles arc (Le Friant et al., 2004), Canary Islands (Mitchell et al., 2003; Llanes et al., 2009), Azores (Quartau et al., 2010) and Aeolian arc (Romagnoli, 2013). We suggest that the shallow shelves around the southern South Sandwich Islands formed in the same way.

The Quaternary global glacially-controlled sea level low stand has a maximum depth of 140 m (Rohling et al., 1998) which controlled insular shallow shelf erosion depths of ca. 120–140 m as observed, for example, in the maximum depths of shallow shelves at Montserrat and in the Aeolian arc (Le Friant et al., 2004; Romagnoli, 2013). Some parts of the shallow shelves around the southern South Sandwich volcanoes are deeper than this global low stand. Much of Longlow Bank, near Montagu Island, is around 380–250 m deep, and much of Harper Bank, near Saunders Island, is 150–200 m deep. The reason for these greater shelf depths is uncertain. It may reflect tectonic subsidence, basal erosion by grounded ice sheets, or abrasion by icebergs. Further uncertainty exists because Quaternary sea level changes in high latitude locations, such as the South Sandwich Islands, are dissimilar from global patterns as a result of gravitational effects of ice sheets and isostatic adjustments; these effects are still poorly constrained for the sub Antarctic (Milne et al., 2009; Roberts et al., 2011). The extent of ice-sheet advance over the South Sandwich shallow shelves during glacial periods is unknown, although the advance of ice sheet to the edges of the more northerly South Georgia shelf (Graham et al., 2008a) suggests that the South Sandwich ice-sheets may have extended to the edges of the shallow shelves. Erosion by iceberg scour, which Hamilton (1989) suggested has modified shallow seamount summits in the area, is unquantified, although the rounded and flattened tops of Orca, Fin and Southern Right seamounts, which cannot have supported ice sheets, may partly be a result of this process. Tectonic subsidence is supported by the deeper submerged banks (Section 4.3), and may also explain shelf-slope breaks of 200–300 m around La Gomera, Canary Islands (Llanes et al., 2009), and we tentatively suggest that this is the cause of the 'deep' shallow shelves around the South Sandwich islands.

Widths of shallow shelves have been correlated with several factors, including age of volcanic construct and dominant wave direction (Le Friant et al., 2004; Llanes et al., 2009). Romagnoli (2013) discussed the factors controlling widths of shallow shelves around the islands of the Aeolian arc and suggested interplay of many processes including edifice age, resistance to erosion, wave regime and relative vertical movements. In the case of the South Sandwich Islands, shelf-slope breaks can be indentified in most directions around all of the islands. Shelf widths from shelf-slope breaks to coasts are generally 1–10 km, the widest being 14 km west of Montagu. Such widths are toward the high end of the range observed around active intraplate and subduction zone volcanic islands (e.g. Le Friant et al., 2004; Llanes et al., 2009; Quartau et al., 2010; Romagnoli, 2013), suggesting relatively high coastal erosion rates consistent with the large Southern Ocean swell (Young, 1999). Because of lack of geochronological data, we are unable to assess shelf width with age of subaerial constructs. Widest shelves tend to be to the north and west, although there is little overall correlation of shelf width with orientation (Fig. 13A). It is therefore uncertain what factors were mainly responsible for producing the wide shelves (Fig. 13B). Prevailing winds are from the west, but only Montagu and Bristol have wide shelves to their west, suggesting that enhanced coastal erosion caused by prevailing waves is not the only controlling factor. Elongation of shelves in an east–west orientation may result from migration of volcanic vents along the direction of minimum principal stress and cross-arc volcanic migration resulting from changes of subducting slab position.

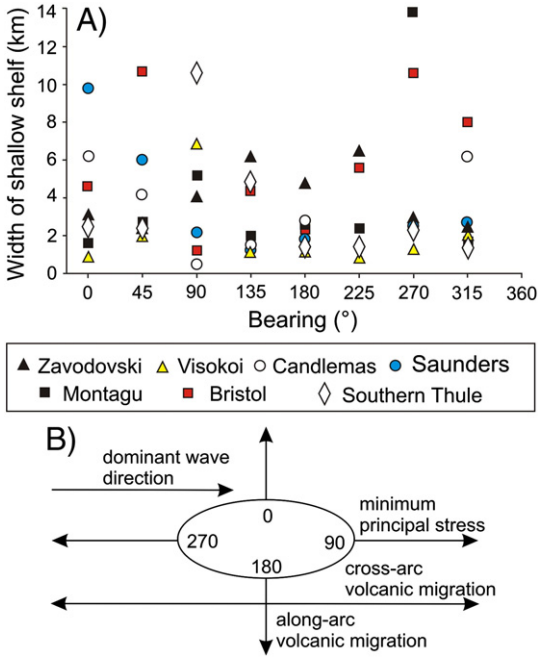

Fig. 13. A. Variation of widths of shallow shelves around volcanic islands of the South Sandwich arc with direction. The shelf edge is usually marked by a slope break around the 250 m isobath. B. Orientation of factors that may contribute to development of shallow shelves.

The wide shelf to the north of Saunders is interpreted as along-arc volcanic migration.

4.3. Submerged banks

The gently sloping Saunders Bank at 750–1100 m depth is a significant feature of the Saunders edifice. Its upper surface is flat and featureless and it is heavily incised on its eastern flank, features that suggest that it is a peneplained erosional remnant, although we do not have seismic or sediment core data to support this interpretation. The alternative explanation that the flat-topped bank was formed by recent submarine volcanic construction is unlikely because of its deep incision. The peneplanation depth of more than 750 m is deeper than global glacial related low sea level stands which have maximum depths of 140 m over the last 0.5 Ma (Rohling et al., 1998). It is also deeper than global sea level at any time during the Pliocene when global climate was warm and sea levels high (Raymo et al., 2011). This suggests that Saunders Bank has subsided up to 1000 m since its peneplanation. A similar submerged bank, Ridge A, which has a flat top and incised eastern flanks, occurs at depths of up to 980 m between Visokoi and Candlemas volcanoes (Leat et al., 2010a). A third is more tentatively identified at a depth of 900–1040 m NE of Adventure. The ages of formation of the volcanic and clastic rocks thought to form these banks and of their peneplanation are not known, so rates of subsidence are unknown. However, their age of formation must be younger than the 10 Ma age of the oceanic crust that is thought to underlie Saunders, Candlemas and Visokoi (Larter et al., 2003).

Subsidence is normal for non-accreting oceanic arcs (Draut and Clift, 2006). Several factors probably contribute to such subsidence, including thermal ageing of the underlying ocean crust, sediment loading, loading resulting from growth of volcanoes by extrusion and intrusion, tectonic extension and fore-arc erosion (Clift and MacLeod, 1999; Waltham et al., 2008). These studies report subsidences of 2–5 km over periods of 20–40 Ma within volcanic arcs adjacent to large volcanoes and close to eroding fore-arcs. The subsidence of up to 1 km of the South Sandwich submerged banks probably is within these rates. The presence of the submerged banks gives a sense of directions of migration of magmatic loci. The distribution of the submerged banks relative to Saunders, Candlemas and Visokoi suggests that the Saunders magmatic locus has migrated south, while Visokoi and Candlemas have migrated apart from a single original locus. In contrast, there are no extensive submerged banks associated with the large southern volcanoes, indicating that their magmatic loci have remained fixed relative to the Sandwich plate.

4.4. Mass-wasting and sedimentary processes

Several mass wasting processes were discussed in relation to the northern volcanoes of the South Sandwich arc by Leat et al. (2010a). Here, we discuss lateral collapse and landslide features: the extensive sediment wave fields around the larger islands and submarine calderas are discussed elsewhere.

4.4.1. Small-scale slide scars

The scars forming linear depressions on seamounts in the north and south Saunders seamount chains are wide in relation to their depth, and flat-bottomed, consistent with origins as small-volume landslide scars. The scars are similar to that on JCR seamount (PS6), Protector Seamounts (Leat et al., 2010a) and transient scars on submarine Monowai volcano, Kermadec arc (Chadwick et al., 2008). The well-surveyed Monowai volcano slide scars formed by repeated down slope movement of unstable largely fragmental material as small-scale landslides and small mass flows (Chadwick et al., 2008). The South Sandwich seamount scars have upper slopes of 18–30° and lower slopes of 14–20°, similar to the Monowai volcano scars, and are interpreted in the same way. The position of the seamounts in the rear-arc, with longer, and therefore possibly less stable, slopes facing the back-arc probably accounts for the location of the small-scale slide scars on their western slopes.

4.4.2. Landslide scars

Large embayments on the slopes of all the large volcanic front volcanoes and some seamounts are interpreted as evidence of larger-scale landsliding. On the larger volcanoes, the landslide scars generally cut into shallow shelves and most extend to depths of ca. 1500–1800 m although some extend deeper. They have steep headwalls and steep inward-facing side walls around 100–200 m high and generally 1.3–6 km apart. Possible compound scars are up to 13 km across. The highly scalloped shallow shelf edges on parts of Candlemas, Bristol, Montagu, and Southern Thule and Adventure indicate a large number of collapse events during volcano evolution. Many of the scars are associated with down-slope sediment waves, and appear to have acted as sediment chutes, and were modified by sediment deposition from small-volume mass flows. Some of the larger landslide scars are partly infilled by constructive volcanism, indicating that evolution of the seamounts and larger volcanic edifices is a complex interaction of volcano growth interspersed with mass wasting events. Importantly, the landslide scars that we observed on the submarine flanks of the subaerial volcanoes are shallow compared to their width and length, forming embayments in plan view. This contrasts with lateral collapse structures both on subaerial volcanoes (Siebert, 1984; Siebert et al., 1987) and on the submarine flanks of many island arc volcanoes (for example, Silver et al., 2009) where lateral collapse scars have sidewalls and headwalls up to 1 km high and up to 25–50% of their width, and where large sectors of volcanoes collapse, often including summit areas. The landslide scars described here have sidewall heights only 2 to 5% of their width. Deeper lateral collapse type scars are seen only on the flanks of a few submarine seamounts in the South Sandwich arc. Hummocky terrains interpreted as debris avalanche deposits are only observed associated with deeper lateral collapses, specifically at Vostok seamount, and associated with the Mount Curry collapse at Zavodovski (Leat et al., 2010a), where they are interpreted to be masked by more recent sedimentation. The absence of such large, deep collapses from the flanks of the subaerial islands (except Zavodovski) is a striking difference between the South Sandwich arc islands and most other island arcs.

4.5. Caldera collapse

Features of calderas discovered in the South Sandwich arc are summarised in Table 2. All the calderas except for the one on Quest Seamount occur on the main volcanic front volcanoes of the southern part of the arc from Montagu to Vysokaya Bank. All are either submarine or ice-filled, and ages of all caldera formations are unknown. All are approximately circular in plan. Caldera walls are well-defined and steep, suggesting well-defined ring faults. Caldera diameters range from 1.6 to 6 km, within the somewhat larger range of caldera diameters recorded in the Tonga–Kermadec (Wright et al., 2006; Massoth et al., 2007; Graham et al., 2008b) and Izu–Bonin (Yuasa et al., 1991; Fiske et al., 2001; Tani et al., 2008) intra-oceanic arcs. Floors of the submarine calderas are imaged as nearly flat, with local mounds that may represent lavas or large hydrothermal mounds. Throws on caldera faults are better constrained for the entirely submarine examples. Estimated caldera volumes range from 0.4–0.9 km^3 for the two nested Quest calderas to 3 km^3 for Resolution and 9–12 km^3 for Douglas Strait, Adventure and Kemp. The Quest volumes are within an order of magnitude of the 0.2 km^3 estimated volume of magma erupted during the dacite–rhyolite eruption of 1962 (Gass et al., 1963; Leat et al., 2007), suggesting that they could have formed during a single similar eruptive event. The larger caldera volumes in the southern volcanoes of the arc may be products of multiple eruptive events as documented for comparable Kermadec arc calderas (Barker et al., 2012).

Table 2
Known calderas in the South Sandwich volcanic arc.

Caldera name	Volcano	Latitude; longitude	Diameter (km)	Depth of caldera floor b.s.l. (m)	Depth of floor below rim (m)	Composition	Activity	Features	References
Quest	Quest Seamount (PS7)	55°49′S 28°31′W	3	870	~130	Intermediate-silicic samples dredges from within caldera	No historical volcanic or hydrothermal activity recorded	Submarine. Nested caldera with inner caldera 1.6 km across by 200 m deep	7, 8, 9
Montagu	Montagu	58°27′S 26°23′W	6	ND	ND	No data on caldera-related products. Lavas from island basaltic-andesitic	Strombolian cone and lava sourced within caldera erupted 2001–2007	Ice-filled	5, 8, 12
Thule	Southern Thule	59°26′S 27°22 W	1.7	ND	ND	No data on caldera-related products	Steam and water observed in crater within caldera 1962	Ice-filled. Forms summit area of Thule Island.	1, 6, 12
Douglas Strait	Southern Thule	59°26′S 27°17′W	5.1 × 4.0	622	~600	Mafic-silicic pre- and post-caldera products	No historical volcanic or hydrothermal activity recorded	Submarine with emergent rims	2, 3, 6
Resolution	Southern Thule	59°26′S 27°03′W	3–4	276	~200	No data on caldera-related products. Bellingshausen Island on N rim is basaltic andesite	Recent volcanism and persistent hydrothermal activity on Bellingshausen Island on N rim. None known within caldera	Submarine with emergent rims	8
Adventure	Vysokaya Bank	59°42′S 27°51′W	5	792	~470	Intermediate-silicic samples dredged from outer slope	No historical volcanic activity recorded. Active hydrothermal vents observed February 2011	Submarine. Flat caldera floor	8, 9
Kemp	Vysokaya Bank	59°41′S 28°20′W	4.3	~1610	~800	Dredge samples from adjacent Kemp Seamount are basalts and basaltic andesites	No historical volcanic activity recorded. Active hydrothermal vents observed February 2009 & February 2010	Submarine. Flat caldera floor	4, 9, 10, 11

ND, no data. References: 1, Holdgate (1963); 2, Smellie et al. (1998); 3, Leat et al. (2003); 4, Leat et al. (2004); 5, Patrick et al. (2005): 6, Allen and Smellie (2008); 7, Leat et al (2010a); 8, Leat et al. (2010b); 9, Author's unpublished data (2011); 10, R.D. Larter et al. unpublished data, and see Supplementary Material S1; 11, Boschen et al. (2013); Patrick and Smellie (2013).

In three cases, rhyolitic and dacitic products are known to be associated with calderas (Table 2), although nowhere has an erupted deposit been stratigraphically linked to caldera formation. It is therefore possible that there is a general association between silicic products and caldera collapse in the South Sandwich arc as well documented in the Tonga–Kermadec (Worthington et al., 1999; Smith et al., 2003; Wright et al., 2006; Graham et al., 2008b; Barker et al., 2012), Izu–Bonin (Fiske et al., 2001; Tani et al., 2008) and Vanuatu (Robin et al., 1993; Monzier et al., 1994) intra-oceanic arcs. Historic volcanic or hydrothermal activity has been observed at most of the South Sandwich calderas (Table 2). Post-caldera volcanism at Montagu has filled most of the caldera, and mafic cinder cones and lavas now rise above the caldera rim (Patrick et al., 2005; Patrick and Smellie, 2013). Post-caldera volcanism at Resolution Caldera has largely occurred on the north rim of the caldera forming the monotonous basaltic andesite volcanics of Bellingshausen Island (Pearce et al., 1995; Leat et al., 2003) which is persistently hydrothermally active. Active submarine hydrothermal vents are known from Adventure and Kemp calderas. The apparent concentration of hydrothermal activity within or adjacent to the calderas is consistent with strong association of hydrothermal plumes with submarine calderas in other intra-oceanic arcs (Baker et al., 2003, 2008; Massoth et al., 2007).

4.6. Latitudinal trends

The volcanic arc forms two distinct sections; a northern section from Saunders northwards, and a southern section including Montagu. The deeper base level in the north is consistent with an oceanic basement (Larter et al., 2003). This section contains the rear-arc seamount chains, consistent with fracturing of oceanic plate, and subsided plateaux, consistent with volcano migration and plate subsidence. The shallower base level in the southern section is consistent with an older, more silicic crustal basement. Preliminary seismic refraction interpretation suggests the presence of an intermediate plutonic middle crust, suggesting that the crust is less oceanic and perhaps proto-continental (Leat et al., 2003). This section has no seamount chains, possibly because of more distributed deformation in the more silicic crust. This section of the arc has larger volcanic front volcanoes and more caldera development, possibly because the thicker and more silicic crust can support larger crustal magma systems.

5. Conclusions

The new multibeam bathymetric coverage confirms that the South Sandwich volcanic arc has a relatively simple structure. A single line of volcanoes forms the well-defined, currently active, convex-east volcanic front. Evidence of one or more parallel, extinct volcanic lines is absent. Topographic evidence for faulting is generally absent, except in the proximity of the trench at both the north and south terminations of the arc. There is no evidence for intra-arc rifting.

1. The northern section of the arc has a deep volcano base level and smaller volcanic front edifice size, consistent with magnetic evidence that it is underlain by oceanic crust. The southern section of the arc has larger volcanoes rising from a shallower base. It is possible that earlier volcanic arc crust underlies much of the southern part of the arc.
2. Three cross-cutting seamount chains extend from the volcanic front for 38–60 km toward the rear-arc, appear to be tectonically controlled, and overlap in age with volcanic front volcanoes.
3. All the volcanic islands are surrounded by 1–10 km wide shallow shelves normally less than 250 m deep, and interpreted to have formed as wave-cut platforms during low sea level stands. Arc subsidence has preserved flat platforms as submerged banks up to 1100 m deep.
4. Landslides and smaller-scale slide scars formed by mass flow are widespread on the flanks of both emergent volcanoes and seamounts. Seamount and volcanic front volcano evolution is a complex

interaction of volcano growth interspersed with major and minor mass wasting events.

5. Seven ice-filled or submarine calderas 1.6–6 km across have been identified in the arc. Six of these represent summit collapse of volcanic front volcanoes in the southern part of the Sandwich plate, where the thicker, possibly more silicic crust is able to support large crustal magma systems. Most have a record of recent hydrothermal or volcanic activity, and most are associated with silicic-intermediate magmatism. The newly discovered Adventure submarine caldera volcano forms the east part of the southernmost main volcano of the volcanic front.

Acknowledgements

This study is part of the British Antarctic Survey Polar Science for Planet Earth Programme and was funded by The Natural Environment Research Council. We are grateful to the officers and crews of the RRS *James Clark Ross* for their support of our science. Participation of S. Day and M. Owen on cruise JR206 was made possible by NERC Antarctic Funding Initiative award CGS-11/58 (2009). We are grateful to Claudia Romagnoli and an anonymous reviewer for detailed and helpful reviews of the paper.

Appendix A. Supplementary data

Supplementary data to this article can be found online at http://dx.doi.org/10.1016/j.jvolgeores.2013.08.013.

References

Allen, C.S., Smellie, J.L., 2008. Volcanic features and the hydrological setting of Southern Thule, South Sandwich Islands. Antarct. Sci. 20, 301–308.
Baker, P.E., 1968. Comparative volcanology and petrology of the Atlantic island-arcs. Bull. Volcanol. 32, 189–206.
Baker, P.E., 1990. South Sandwich Islands. In: LeMasurier, W.E., Thomson, J.W. (Eds.), Volcanoes of the Antarctic Plate and Southern Oceans, Antarctic Research Series 48. AGU, Washington, D.C., pp. 361–395.
Baker, P.E., Buckley, F., Rex, D.C., 1977. Cenozoic volcanism in the Antarctic. Philos. Trans. R. Soc. Lond. B 279, 131–142.
Baker, E.T., Feeley, R.A., de Ronde, C.E.J., Massoth, G.J., Wright, I.C., 2003. Submarine hydrothermal venting on the southern Kermadec volcanic arc front (offshore New Zealand): location and extent of particle plume signatures. In: Larter, R.D., Leat, P.T. (Eds.), Intra-Oceanic Subduction Systems: Tectonic and Magmatic Processes. Geological Society, London Special Publications, 219, pp. 141–161.
Baker, E.T., Embley, R.W., Walker, S.L., Resing, J.A., Lupton, J.E., Nakamura, K., de Ronde, C.E.J., Massoth, G.J., 2008. Hydrothermal activity and volcano distribution along the Mariana arc. J. Geophys. Res. 113, B08S09. http://dx.doi.org/10.1029/2007JB005423.
Barker, P.F., 1995. Tectonic framework of the East Scotia Sea. In: Taylor, B. (Ed.), Backarc Basins: Tectonics and Magmatism. Plenum Press, New York, pp. 281–314.
Barker, S.J., Rotella, M.D., Wilson, C.J.N., Wright, I.C., Wysoczanski, R.J., 2012. Contrasting pyroclast density spectra from subaerial and submarine silicic eruptions in the Kermadec arc: implications for eruption processes and dredge sampling. Bull. Volcanol. 74, 1425–1443.
Boschen, R.E., Tyler, P.A., Copley, J.T., 2013. Distribution, population structure, reproduction and diet of *Ophiolimna antarctica* (Lyman, 1879) from Kemp Caldera in the Southern Ocean. Deep Sea Res. Part II 92, 27–35.
Chadwick, W.W., Wright, I.C., Schwarz-Schamera, U., Hyvernaud, O., Reymond, D., de Ronde, C.E.J., 2008. Cyclic eruptions and sector collapses at Monowai submarine volcano, Kermadec arc: 1998–2007. Geochem. Geophys. Geosyst. 9, Q10014. http://dx.doi.org/10.1029/2008GC002113.
Clift, P.D., MacLeod, C.J., 1999. Slow rates of subduction erosion estimated from subsidence and tilting of the Tonga forearc. Geology 27, 411–414.
Dragani, W.C., D'Onofrio, E.E., Grismeyer, W., Fiore, M.M.E., Violante, R.A., Rovere, E.I., 2009. Vulnerability of the Atlantic Patagonian coast to tsunamis generated by submarine earthquakes located in the Scotia Arc region. Some numerical experiments. Nat. Hazard. 49, 437–458.
Draut, A.E., Clift, P.D., 2006. Sedimentary processes in modern and ancient oceanic arc settings: evidence from the Jurassic Talkeetna Formation of Alaska and the Mariana and Tonga arcs, Western Pacific. J. Sediment. Res. 76, 493–514.
Fiske, R.S., Naka, J., Iizasa, K., Yuasa, M., Klaus, A., 2001. Submarine silicic caldera at the front of the Izu–Bonin arc, Japan: voluminous seafloor eruptions of rhyolite pumice. Bull. Geol. Soc. Am. 113, 813–824.
Forsyth, D.W., 1975. Fault plane solutions and tectonics of the South Atlantic and Scotia Sea. J. Geophys. Res. 80, 1429–1443.
Gass, I.G., Harris, P.G., Holdgate, M.W., 1963. Pumice eruption in the area of the South Sandwich Islands. Geol. Mag. 100, 321–330.
Graham, A.G.C., Fretwell, P.T., Larter, R.D., Hodgson, D.A., Wilson, C.K., Tate, A.J., Morris, P., 2008a. A new bathymetric compilation highlighting extensive paleo-ice sheet drainage on the continental shelf, South Georgia, sub-Antarctica. Geochem. Geophys. Geosyst. 9, Q07011. http://dx.doi.org/10.1029/2008GC001993.
Graham, I.J., Reyes, A.G., Wright, I.C., Peckett, K.M., Smith, I.E.M., Arculus, R.J., 2008b. Structure and petrology of newly discovered volcanic centres in the northern Kermadec-southern Tofua arc, South Pacific Ocean. J. Geophys. Res. 113, B08S02. http://dx.doi.org/10.1029/2007JB005453.
Hamilton, I.W., 1989. Geophysical investigations of subduction-related processes in the Scotia Sea. (Ph.D. Thesis) Univ. Birmingham, UK.
Holdgate, M.W., 1963. Observations in the South Sandwich Islands, 1962. Polar Rec. 11 (73), 394–405.
Holdgate, M.W., Baker, P.E., 1979. The South Sandwich Islands: I. General description. British Antarctic Survey Scientific Reports No. 91.
Ishizuka, O., Uto, K., Yuasa, M., 2003. Volcanic history of the back-arc region of the Izu–Bonin (Ogasawara) arc. In: Larter, R.D., Leat, P.T. (Eds.), Intra-Oceanic Subduction Systems: Tectonic and Magmatic Processes. Geological Society, London Special Publications, 219, pp. 187–205.
Ishizuka, O., Geshi, N., Itoh, J., Kawanabe, Y., TuZino, T., 2008. The magmatic plumbing of the submarine Hachijo NW volcanic chain, Hachijojima, Japan: long-distance magma transport? J. Geophys. Res. 113, B08S08. http://dx.doi.org/10.1029/2007JB005325.
Kaiser, S., Barnes, D.K.A., Linse, K., Brandt, A., 2008. Epibenthic macrofauna associated with the shelf and slope of a young and isolated Southern Ocean island. Antarct. Sci. 20, 281–290.
Kaneko, T., Yasuda, A., Shimano, T., Nakada, S., Fujii, T., Kanazawa, T., Nishizawa, A., Matsumoto, Y., 2005. Submarine flank eruption preceding caldera subsidence during the 2000 eruption of Miyakejima volcano, Japan. Bull. Volcanol. 67, 243–253.
Lachlan-Cope, T., Smellie, J.L., Ladkin, R., 2001. Discovery of a recurrent lava lake on Saunders Island (South Sandwich Islands) using AVHRR imagery. J. Volcanol. Geotherm. Res. 112, 105–116.
Larter, R.D., Vanneste, L.E., Morris, P., Smyth, D.K., 2003. Structure and tectonic evolution of the South Sandwich arc. In: Larter, R.D., Leat, P.T. (Eds.), Intra-Oceanic Subduction Systems: Tectonic and Magmatic Processes. Geological Society, London Special Publications, 219, pp. 255–284.
Le Friant, A., Harford, C.L., Deplus, C., Boudon, G., Sparks, R.S.J., Herd, R.A., Komorowski, J.C., 2004. Geomorphological evolution of Montserrat (West Indies): importance of flank collapse and erosional processes. J. Geol. Soc. Lond. 161, 147–160.
Leat, P.T., Smellie, J.L., Millar, I.L., Larter, R.D., 2003. Magmatism in the South Sandwich arc. In: Larter, R.D., Leat, P.T. (Eds.), Intra-Oceanic Subduction Systems: Tectonic and Magmatic Processes. Geological Society, London Special Publications, 219, pp. 285–313.
Leat, P.T., Pearce, J.A., Barker, P.F., Millar, I.L., Barry, T.L., Larter, R.D., 2004. Magma genesis and mantle flow at a subducting slab edge: the South Sandwich arc-basin system. Earth Planet. Sci. Lett. 227, 17–35.
Leat, P.T., Larter, R.D., Millar, I.L., 2007. Silicic magmas of Protector Shoal, South Sandwich arc: indicators of generation of primitive continental crust in an island arc. Geol. Mag. 144, 179–190.
Leat, P.T., Tate, A.J., Tappin, D.R., Day, S.J., Owen, M.J., 2010a. Growth and mass wasting of volcanic centers in the northern South Sandwich arc, revealed by new multibeam mapping. Mar. Geol. 275, 110–126.
Leat, P.T., Tate, A.J., Deen, T.J., Day, S.J., Owen, M.J., 2010b. RRS James Clark Ross JR206 cruise report: volcanic and continental slope processes, South Georgia and South Sandwich Islands. British Antarctic Survey Cruise Report ES6/1/2010/1.
Livermore, R., 2003. Back-arc spreading and mantle flow in the East Scotia Sea. In: Larter, R.D., Leat, P.T. (Eds.), Intra-Oceanic Subduction Systems: Tectonic and Magmatic Processes. Geological Society, London Special Publications, 219, pp. 315–331.
Livermore, R., Cunningham, A., Vanneste, L., Larter, R., 1997. Subduction influence on magma supply at the East Scotia Ridge. Earth Planet. Sci. Lett. 150, 261–275.
Llanes, P., Herrera, R., Gómez, M., Muñoz, A., Acosta, J., Uchupi, E., Smith, D., 2009. Geological evolution of the volcanic island La Gomera, Canary Islands, from analysis of its geomorphology. Mar. Geol. 264, 123–139.
Machida, S., Ishii, T., Kimura, J.-I., 2008. Petrology and geochemistry of cross-chaINS in the Izu–Bonin back-arc: three mantle components with contributions of hydrous liquids from a deeply subducted slab. Geochem. Geophys. Geosyst. 9, Q05002. http://dx.doi.org/10.1029/2007GC001641.
Massoth, G., Baker, E., Worthington, T., Lupton, J., de Ronde, C., Arculus, R., Walker, S., Nakamura, K., Ishibashi, J., Stoffers, P., Resing, J., Greene, R., Lebon, G., 2007. Multiple hydrothermal sources along the south Tonga arc and Valu Fa Ridge. Geochem. Geophys. Geosyst. 8, Q11008. http://dx.doi.org/10.1029/2007GC001675.
Milne, G.A., Gehrels, W.R., Hughes, C.W., Tamisiea, M.E., 2009. Identifying the causes of sea-level change. Nat. Geosci. 2, 471–478.
Mitchell, N.C., Dade, W.B., Masson, D.G., 2003. Erosion of the submarine flanks of the Canary Islands. J. Geophys. Res. 108 (F1), 6002. http://dx.doi.org/10.1029/2002JF000003.
Monzier, M., Robinm, C., Eissen, J.P., 1994. Kuwae (≈1425 A.D.): the forgotten caldera. J. Volcanol. Geotherm. Res. 59, 207–218.
Oakley, A.J., Taylor, B., Moore, G.F., Goodliffe, A., 2009. Sedimentary, volcanic, and tectonic processes of the central Mariana arc: Mariana back-arc basin formation and the West Mariana Ridge. Geochem. Geophys. Geosyst. 10, Q08X07. http://dx.doi.org/10.1029/2008GC002312.
Hydrographic Office, 2003. South Sandwich Islands, Chart No. 3593, 1:500 000. Admiralty Hydrographic Department, Taunton.
Okal, E.A., Hartnady, C.J., 2009. The South Sandwich Islands earthquake of 27 June 1929: seismological study and inference on tsunami risk for the South Atlantic. S. Afr. J. Geol. 112, 359–370.
Patrick, M.R., Smellie, J.L., 2013. A spaceborne inventory of volcanic activity in Antarctica and southern oceans, 2000–10. Antarct. Sci. 25, 475–500.
Patrick, M.R., Smellie, J.L., Harris, A.J.L., Wright, R., Dean, K., Izbekov, P., Garbeil, H., Pilger, E., 2005. First recorded eruption of Mount Belinda volcano (Montagu Island), South Sandwich Islands. Bull. Volcanol. 67, 415–422.

Pearce, J.A., Baker, P.E., Harvey, P.K., Luff, I.W., 1995. Geochemical evidence for subduction fluxes, mantle melting and fractional crystallization beneath the South Sandwich island arc. J. Petrol. 36, 1073–1109.
Quartau, R., Trenhaile, A.S., Mitchell, N.C., Tempera, F., 2010. Development of volcanic insular shelves: insights from observations and modelling of Faial Island in the Azores Archipelago. Mar. Geol. 275, 66–83.
Raymo, M.E., Mitroica, J.X., O'Leary, M.J., DeConto, R.M., Hearty, P.J., 2011. Departures from eustasy in Pliocene sea-level records. Nat. Geosci. 4, 328–332.
Roberts, S.J., Hodgson, D.A., Sterken, M., Whitehouse, P.L., Verleyen, E., Vyverman, W., Sabbe, K., Balbo, A., Bentley, M.J., Moreton, S.G., 2011. Geological constraints on glacio-isostatic adjustment models of relative sea-level change during deglaciation of Prince Gustav Channel, Antarctic Peninsula. Quat. Sci. Rev. 30, 3603–3617.
Robin, C., Eissen, J.-P., Monzier, M., 1993. Giant tuff cone and 12 km-wide associated caldera at Ambrym Volcano (Vanuatu, New Hebrides arc). J. Volcanol. Geotherm. Res. 55, 225–238.
Rogers, A.D., Tyler, P.A., Connelly, D.P., Copley, J.T., James, R., et al., 2012. The discovery of new deep-sea hydrothermal vent communities in the Southern Ocean and implications for biogeography. PLoS Biol. 10 (1), e1001234. http://dx.doi.org/10.1371/journal.pbio.1001234.
Rohling, E.J., Fenton, M., Jorissen, F.J., Bertrand, P., Ganssen, G., Caulet, J.P., 1998. Magnitudes of sea-level lowstands of the past 500,000 years. Nature 394, 162–165.
Romagnoli, C., 2013. Characteristics and morphological evolution of the Aeolian volcanoes from the study of submarine portions. In: Lucchi, F., Peccerillo, A., Keller, J., Tranne, C.A., Rossi, P.L. (Eds.), The Aeolian Islands Volcanoes. Geological Society, London, Memoirs, 37, pp. 13–26 (http://dx.doi.org/10.1144/M37.3).
Siebert, L., 1984. Large volcanic debris avalanches: characteristics of source areas, deposits, and associated eruptions. J. Volcanol. Geotherm. Res. 22, 163–197.
Siebert, L., Glicken, H., Ui, T., 1987. Volcanic hazards from Bezymianny- and Bandai-type eruptions. Bull. Volcanol. 49, 435–459.
Silver, E., Day, S., Ward, S., Hoffmann, G., Llanes, P., Driscoll, N., Appelgate, B., Saunders, S., 2009. Volcano collapse and tsunami generation in the Bismarck Volcanic Arc, Papua New Guinea. J. Volcanol. Geotherm. Res. 186, 210–222.
Smellie, J.L., Morris, P., Leat, P.T., Turner, D.B., Houghton, D., 1998. Submarine caldera and other volcanic observations in Southern Thule, South Sandwich Islands. Antarct. Sci. 10, 171–172.
Smith, I.E.M., Worthington, J., Stewart, R.B., Price, R.C., Gamble, J.A., 2003. Felsic volcanism in the Kermadec arc, SW Pacific: crustal recycling in an oceanic setting. In: Larter, R.D., Leat, P.T. (Eds.), Intra-Oceanic Subduction Systems: Tectonic and Magmatic Processes. Geological Society, London Special Publications, 219, pp. 99–118.
Stern, R.J., Jackson, M.C., Fryer, P., Ito, E., 1993. O, Sr, Nd and Pb isotopic composition of the Kasuga cross-chain in the Mariana arc: a new perspective on the K–*h* relationship. Earth Planet. Sci. Lett. 119, 459–475.
Stern, R.J., Kohut, E., Bloomer, S.H., Leybourne, M., Fouch, M., Vervoot, J., 2006. Subduction factory processes beneath the Guguan cross-chain, Mariana arc: no role for sediments, are sepentinites important? Contrib. Mineral. Petrol. 151, 202–221.
Tani, K., Fiske, R.S., Tamura, Y., Kido, Y., Naka, J., Shukuno, H., Takeuchi, R., 2008. Sumisu volcano, Izu–Bonin arc, Japan: site of a silicic caldera-forming eruption from a small open-ocean island. Bull. Volcanol. 70, 547–562.
Tate, A.J., Leat, P.T., 2007. RRS James Clark Ross JR168 cruise report: swath bathymetry South Sandwich Islands. British Antarctic Survey Cruise Report ES6/1/2007/1. (16 pp.).
Taylor, R.N., Nesbitt, R.W., 1998. Isotopic characteristics of subduction fluids in an intra-oceanic setting, Izu–Bonin arc, Japan. Earth Planet. Sci. Lett. 164, 79–98.
Thomas, C., Livermore, R.A., Pollitz, F.F., 2003. Motion of the Scotia Sea plates. Geophys. J. Int. 155, 789–804.
Todd, E., Gill, J.B., Wysoczanski, R.J., Handler, M.R., Wright, I.C., Gamble, J.A., 2010. Sources of constructional cross-chain volcanism in the southern Havre Trough: new insights from HFSE and REE concentration and isotope systematics. Geochem. Geophys. Geosyst. 11, Q04009. http://dx.doi.org/10.1029/2009GC002888.
Tonarini, S., Leeman, W.P., Leat, P.T., 2011. Subduction erosion of forearc mantle wedge implicated in the genesis of the South Sandwich Island (SSI) arc: evidence from boron isotope systematic. Earth Planet. Sci. Lett. 301, 275–284.
Vanneste, L.E., Larter, R.D., 2002. Sediment subduction, subduction erosion, and strain regime in the northern South Sandwich forearc. J. Geophys. Res. 107 (B7), 2149. http://dx.doi.org/10.1029/2001JB000396.
Waltham, D., Hall, R., Smyth, H.R., Ebinger, C.J., 2008. Basin formation by volcanic arc loading. Geol. Soc. Am. Spec. Pap. 436, 11–26.
Wilson, M., 1989. Igneous Petrogenesis. Unwin Hyman, London.
Worthington, T.J., Gregory, M.R., Bondarenko, V., 1999. The Denham caldera on Raoul Volcano: dacitic volcanism in the Tonga–Kermadec arc. J. Volcanol. Geotherm. Res. 90, 29–48.
Wright, I.C., Parson, L.M., Gamble, J.A., 1996. Evolution and interaction of migrating cross-chain volcanism and back-arc rifting: an example from the southern Havre Trough. J. Geophys. Res. 101, 22071–22086.
Wright, I.C., Worthington, T.J., Gamble, J.A., 2006. New multibeam mapping and geochemistry of the 30°–35°S sector, and overview, of southern Kermadec arc volcanism. J. Volcanol. Geotherm. Res. 149, 263–296.
Wysoczanski, R.J., Todd, E., Wright, I.C., Leybourne, M.I., Hergt, J.M., Adam, C., Mackay, K., 2010. Backarc rifting, constructional volcanism and nascent disorganised spreading in the southern Havre Trough Backarc rifts (SW Pacific). J. Volcanol. Geotherm. Res. 190, 39–57.
Young, I.R., 1999. Seasonal variability of the global ocean wind and wave climate. Int. J. Climatol. 19, 931–950.
Yuasa, M., Murakami, F., Saito, E., Watanabe, K., 1991. Submarine topography of seamounts on the volcanic front of the Izu–Ogasawara (Bonin) arc. Bull. Geol. Soc. Jpn. 42, 703–743.